

Uncertainty and causal emergence in complex networks

Brennan Klein^{*1,2} and Erik Hoel^{†3}

¹*Network Science Institute, Northeastern University, Boston, MA, USA*

²*Laboratory for the Modeling of Biological and Socio-Technical Systems, Northeastern University, Boston, USA*

³*Allen Discovery Center, Tufts University, Medford, MA, USA*

August 2, 2021

Abstract

The connectivity of a network conveys information about the dependencies between nodes. We show that this information can be analyzed by measuring the uncertainty (and certainty) contained in paths along nodes and links in a network. Specifically, we derive from first principles a measure known as *effective information* and describe its behavior in common network models. Networks with higher effective information contain more information within the dependencies between nodes. We show how subgraphs of nodes can be grouped into macro-nodes, reducing the size of a network while increasing its effective information, a phenomenon known as causal emergence. We find that causal emergence is common in simulated and real networks across biological, social, informational, and technological domains. Ultimately, these results show that the emergence of higher scales in networks can be directly assessed, and that these higher scales offer a way to create certainty out of uncertainty.

Introduction

Networks provide a powerful syntax for representing a wide range of systems, from the trivially simple to the highly complex [1, 2, 3]. It is common to characterize networks based on structural properties like their degree distribution or whether they show community structure. While our understanding of these structural properties of networks has been crucial for the rapid rise of network science as a discipline, there is a distinct gap in our treatment of both dependencies between nodes and also higher scales in networks. This gap is especially pressing because networks often have an interpretation where links represent dependencies, such as contact networks in epidemiology [4], neuronal and functional networks in the brain [5], or interaction networks among cells, genes, or drugs [6], and these networks can often be analyzed at multiple different scales.

Previously, others have used directed acyclic graphs known as “causal diagrams” [7, 8] to represent causal relationships as dependencies in networks. But there has been little research on quantifying or broadly classifying such causation in networks, particularly those that have both weighted connections and feedback, which are hallmarks of complex systems across domains [9, 10]. Here we introduce information-theoretic measures designed to capture the information contained in the dependencies of networks and which can be used to identify when these networks possess informative higher scales.

Describing cause and effect implicitly invokes the idea of a network. For example, if a system in a particular state, A , always transitions to state B , the causal relationship between A and B can be represented by a node-link diagram wherein the two nodes— A and B —are connected by a directed arrow, indicating that B depends on A . In such a network, the out-weight vector, W_i^{out} , of a node, v_i , represents the possible

*klein.br@northeastern.edu

†erik.hoel@tufts.edu

transitions and their probabilities from that node. Specifically, W_i^{out} consists of weights w_{ij} between node v_i and its neighbors v_j , where $w_{ij} = 0.0$ if there is no edge from v_i to v_j . This means the edge weights w_{ij} can be interpreted as the probability p_{ij} that a random walker on v_i will transition to v_j in the next time step. We will refer to such a network as having a *causal structure*.

In the cases where links between nodes represent dependency in general, such as influence, strength, or potential causal interactions, but not explicitly transitions (or where details about transitions is lacking), for our analysis we create W_i^{out} by normalizing each node’s out-weight vector to sum to 1.0. This generalizes our results to multiple types of representations (although what sort of dependencies the links in the network represent should be kept in mind when interpreting the values of the measures we introduce below).

A network’s causal structure can be characterized by the uncertainty in the relationships among the nodes’ out-weights (possible effects) and in-weights (possible causes). The total information in the dependencies between nodes is a function of this uncertainty and can be derived from two fundamental properties. The first is the uncertainty of a node’s effects, which can be quantified by the Shannon entropy [11] of its out-weights, $H(W_i^{out})$. The average of this entropy, $\langle H(W_i^{out}) \rangle$, across all nodes is the amount of noise present in the network’s causal structure. Only if $\langle H(W_i^{out}) \rangle$ is zero is the network is *deterministic*.

The second fundamental causal property is how weight is distributed across the whole network, $\langle W_i^{out} \rangle$. This vector $\langle W_i^{out} \rangle$ consists of elements that are the sum of the in-weights w_{ji} to each node v_i from each of its incoming neighbors, v_j (then normalized by total weight of the network). Its entropy, $H(\langle W_i^{out} \rangle)$, reflects how certainty is distributed across the network. If all nodes link only to the same node, then $H(\langle W_i^{out} \rangle)$ is zero, and the network is totally *degenerate* since all causes lead to the same effect.

From these two properties we can derive the amount of information in a network’s causal structure, the *effective information* (EI), as:

$$EI = H(\langle W_i^{out} \rangle) - \langle H(W_i^{out}) \rangle \tag{1}$$

Here, we use this measure to develop a general classification of networks (key terms and definitions can be found in the Supplementary Materials, SM 1.1). Networks with high EI contain more certainty in the relationships between nodes in the network (since the links represent greater dependencies), whereas networks with low EI contain less certainty.

In this work, we show how the connectivity and different growth rules of a network have a deep relationship to that network’s EI . This also provides a principled means of quantifying the amount of information among the micro-, meso-, and macroscale dependencies in a network. We introduce a formalism for finding and assessing the most informative scale of a network: the scale that minimizes the uncertainty in the dependencies between nodes. For some networks, a macroscale description of the network can be more informative in this manner, demonstrating a phenomenon known as *causal emergence* [12, 13]. This provides a rigorous means of identifying when networks possess an informative higher scale.

Results

Effective information quantifies a network’s dependencies

Our work in networks expands previous research on using information theory to measure dependencies. A version of EI designed to capture the causal influence between two subsets of neurons was originally introduced as a step in the calculation of integrated information in the brain [14]. Later, a system-wide version of EI was shown to capture fundamental causal properties in logic gates, particularly their determinism and degeneracy [12]. Our derivation from first principles of an EI for networks is equivalent to this system-wide definition (SM 1.2).

It is important to know how EI behaves in standard network models and their growth. Here we examine the EI of different common network structures, asking basic questions about the relationship between a network’s EI and its size, density, and structure. These inquiries allow for the exhaustive classification and quantification of the information contained in the dependencies of real networks. It is intuitive that the EI of a network will increase as the network grows in size. In general, adding more nodes should increase the

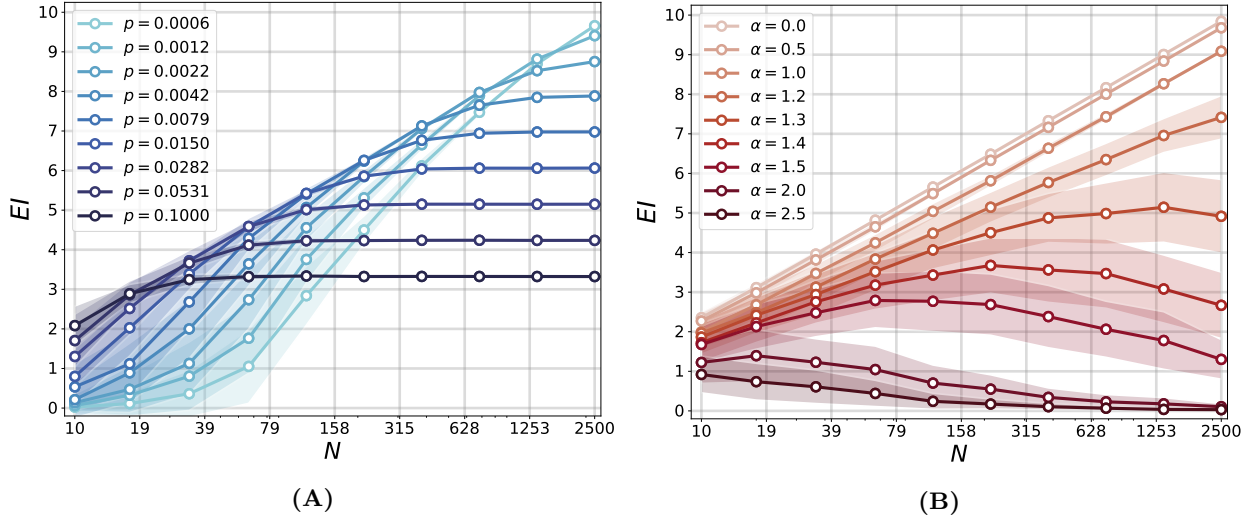


Figure 1: Effective information depends on network structure. (A) In Erdős-Rényi (ER) networks we see the network’s EI level off at $EI = -\log_2(p)$ as N , the network’s size, increases (log scale shown). (B) The EI of networks grown under a preferential attachment mechanism, which depends on the preferential attachment exponent, α . Under this network growth model, new nodes add their m edges (here, $m = 1$) to existing nodes in the network with a probability proportional to k^α . Only superlinear preferential attachment ($\alpha > 1.0$) allows for the continuous growth of EI with the growth of the network. In A and B, the ribbon around each line represents standard deviation after 100 simulations of each.

available repertoire of counterfactuals, states, or causes (depending on what exactly the nodes represent), which should in turn increase the amount of information. However, in cases of randomness rather than structure, EI should reflect this randomness. We found this is indeed the case.

In Figure 1A, we show the relationship between a network’s EI and its size under several parameterizations of Erdős-Rényi (ER) random graphs [15, 16]. As the size of an ER network increases (while keeping constant the probability that any two nodes will be connected, p), its EI converges to a value of $-\log_2(p)$. That is, in random networks EI is dominated solely by the probability that any two nodes are connected, a key finding which demonstrates that, after a certain point, a random causal structure does not contain more information as its size increases. This shift occurs in ER networks at approximately $\langle k \rangle = \log_2(N)$, which is also the point at which we can expect all nodes to be in a giant component [1]. This finding proves that network connectivity must be non-random to increase the amount of information in the dependencies between nodes (see SM 1.3.1 for derivation). Note that if a network is maximally dense (i.e. a fully connected network, with self-loops), $EI = 0.0$. However, we expect such dense low- EI structures to be uncommon, since network structures found in nature and society tend to be sparse [17].

We report another fundamental relationship between a network’s connectivity and its EI in Figure 1B. We again compare the EI of a network to its size, focusing on networks grown under different parameterizations of a preferential attachment model. Under a preferential attachment growth model, a new node is added to the network at each time step, contributing m new edges to the network; these m edges connect to nodes already in the network, v_j , with a probability proportional to k_j^α . Here k_j is the degree of node v_j and α tunes the amount of preferential attachment. A value of $\alpha = 0.0$ corresponds to each node having an equal chance of receiving a new node’s link (i.e., no preferential attachment). The classic Barabási-Albert network corresponds to linear preferential attachment, $\alpha = 1.0$ [18]. Superlinear preferential attachment, $\alpha > 1.0$, creates networks that have less and less EI , eventually resembling star-like structures (see SM 1.3.2 for derivation). As shown in Figure 1B, only in cases of sublinear preferential attachment, $\alpha < 1.0$, does the network’s EI increase with its size. When $\alpha = 0.0$ —creating a random tree—the network’s EI increases

logarithmically as its size increases.

The maximum possible EI in a network of N nodes is $\log_2(N)$. This can be seen in the case of a directed ring network where each node has one incoming link and one outgoing link, each with a weight of 1.0, so each node has one node uniquely dependent on it. In such a network, each node contributes zero uncertainty, since $\langle H(W_i^{out}) \rangle = 0.0$, and $H(\langle W_i^{out} \rangle) = \log_2(N)$, and therefore its EI is always $\log_2(N)$. In general, the EI of undirected lattices is fixed entirely by its size and the dimension of the ring lattice (i.e. $d = 1$ is an undirected ring, $d = 2$ is a taurus, etc. [19]), so for such lattices $EI = \log_2(N) - \log_2(2d)$ (see SM 1.3.2 for derivation).

The picture that emerges is that EI is inextricably linked a network’s connectivity and growth, and therefore to the fundamentals of network science (even network motifs, as shown in SM 1.4). Random networks have a fixed amount of EI , and scale-freeness ($\alpha = 1.0$) represents the critical bound for the growth of EI . In general, dense networks and star-like networks have less EI . The next section explores how EI ’s components explain these associations.

Determinism and degeneracy

Determinism and *degeneracy* are the two fundamental components of EI [12]. They govern the degree of certainty in the causal relationships of a system and, as we show here, are based on a network’s connectivity. A visual explanation of these two quantities are shown in Figure 2A. Being fundamental to causality, the two properties are derivable from the uncertainty over outputs and uncertainty in how those outputs are distributed, respectively:

$$\text{determinism} = \log_2(N) - \langle H(W_i^{out}) \rangle \quad (2)$$

$$\text{degeneracy} = \log_2(N) - H(\langle W_i^{out} \rangle) \quad (3)$$

In a maximally deterministic system wherein all nodes have a single output, $w_{ij} = 1.0$, the determinism is just $\log_2(N)$ because $\langle H(W_i^{out}) \rangle = 0.0$. Degeneracy is the amount of information in the dependencies lost via an overlap in input weights (e.g., if multiple nodes output to the same node). In a perfectly non-degenerate system wherein all nodes have an equal input weight, the degeneracy is zero because $H(\langle W_i^{out} \rangle) = \log_2(N)$. Together, determinism and degeneracy can be used to define EI , wherein:

$$EI = \text{determinism} - \text{degeneracy} \quad (4)$$

These two quantities provide clear explanations for why different networks have the EI they do. For example, as the size of an Erdős-Rényi random network increases, its degeneracy approaches zero, which means the EI of a random network is driven only by the determinism of the network, which is in turn the negative log of the probability of connection, p . Similarly, in d -dimensional ring lattice networks, the degeneracy term is always zero, which means the EI of a ring lattice structure also reduces to the determinism of that structure. Ring networks with an average degree $\langle k \rangle$ will have a higher EI than ER networks with the same average degree because ring networks will have a higher determinism value. In the case of star networks, the degeneracy term alone governs the decay of the EI such that hub-and-spoke-like structures quickly become uninformative in terms of cause and effect (see SM 1.3 for derivations concerning these cases). In general, this means that canonical networks can be characterized by their ratio of determinism to degeneracy (see Fig 2B).

Effective information in real networks

EI often grows with network size. To compare networks of different sizes, we examine their *effectiveness*, which is the EI normalized by the size of the network to a value between 0.0 and 1.0:

$$\text{effectiveness} = \frac{EI}{\log_2(N)} \quad (5)$$

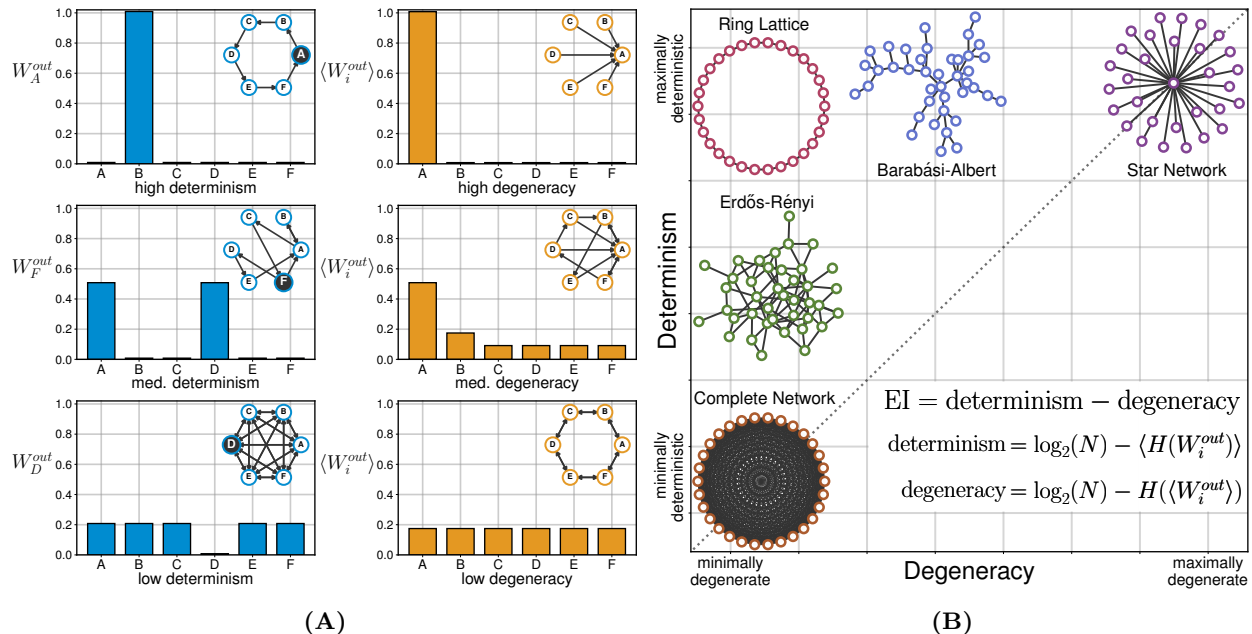


Figure 2: Comparing determinism and degeneracy. (A) Left column: three example out-weight vectors, W_i^{out} , of a given node, v_i . A maximally deterministic vector (top left, where the W_A^{out} corresponds to node A in the inset network motif) is when a random walker on v_i transitions to one of its neighbors with probability 1.0, whereas indeterminism occurs when v_i has a uniform probability of visiting any node in the network in the next time step. Right: three example in-weight vectors to a given v_j . A maximally degenerate vector, $\langle W_i^{out} \rangle$ (top right, exemplified by the inset network motif), is when every outgoing edge in the network connects to a single node, whereas minimal degeneracy occurs when each value in $\langle W_i^{out} \rangle$ is uniformly $\frac{1}{N}$. (B) By comparing the determinism and degeneracy of canonical network structures, we find a great deal of heterogeneity in different network models' ratios between their determinism and degeneracy. High degeneracy is characterized by hub-and-spoke topology, as in the case of the star network. Networks with high determinism are characterized by longer average path lengths, as in the case of a ring lattice.

As the noise and/or the degeneracy of a network increases toward their upper possible bounds, the effectiveness of that network will trend to 0.0. Regardless of its size, a network wherein each node has a deterministic output to a unique target has an effectiveness of 1.0.

In Figure 3, we examine the effectiveness of 84 different networks corresponding to data from real systems. These networks were selected primarily from the Konect Network Database [20], which was used because its networks are publicly available, range in size from dozens to tens of thousands of nodes, often have a reasonable interpretation as a causal structure, and they are diverse, ranging from social networks, to power networks, to metabolic networks. We defined four categories of interest: biological, social, informational, and technological. We selected our networks by using all the available networks (under 40,000 nodes due to computational constraints) in the domains corresponding to each category within the Konect database, and where it was appropriate, the Network Repository as well [21]. See the Materials & Methods section and SM Table 2 for a full description of this selection process.

Lower effectiveness values correspond to structures that either have high degeneracy (as in right column, Figure 2A), low determinism (as in left column, Figure 2A), or a combination of both. In the networks we measured, biological networks on average have lower effectiveness values, whereas technological networks on average have the highest effectiveness. This finding aligns intuitively with what we know about the relationship between EI and network structure, and it also supports long-standing hypotheses about the role of redundancy, degeneracy, and noise in biological systems [22, 23]. On the other hand, technological networks

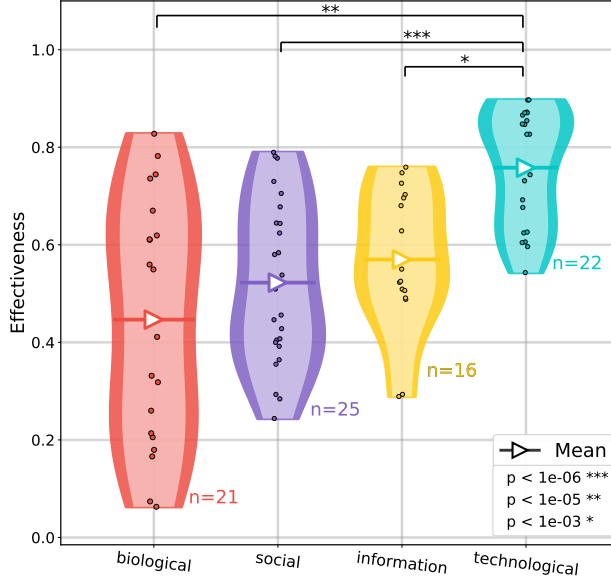


Figure 3: Effective information of real networks. Effectiveness—a network’s EI , normalized by $\log_2(N)$ [12]—of 84 real networks from the Konect network database [20], grouped by domain of origin. To look further at the names and domains of the networks in question, see SM 1.5. Networks in different categories have varying effectiveness (t-test, comparison of means).

such as power grids, autonomous systems, or airline networks are associated with higher effectiveness values on average. One explanation for this difference is that efficiency in human-made technological networks tends to create sparser, non-degenerate networks with higher effectiveness on average.

Perhaps it might be surprising to find that evolved networks have such low effectiveness. But, as we will show, a low effectiveness can actually indicate that there are informative higher-scale (macroscale) dependencies in the system. That is, a low effectiveness can be reflective of the fact that biological systems often contain higher-scale causal structure, which we demonstrate in the following section.

Causal emergence in complex networks

This new global network measure, EI , offers a principled way to answer an important question: what is the scale that best captures the dependencies in a complex system?

The resolution to this question is important because science analyzes the causal structure of different systems at different spatiotemporal scales, often preferring to intervene and observe systems at levels far above that of the microscale [13]. This is likely because causal relationships at the microscale can be extremely noisy and therefore uninformative, and coarse-graining can minimize this noise [12]. Indeed, this noise minimization is actually grounded in Claude Shannon’s noisy-channel coding theorem [11], wherein dimension reductions can operate like codes that use more of a channel’s capacity [24]. Higher-level causal relationships often perform error-correction on the lower-level relationships, thus generating extra effective information at those higher scales. Measuring this difference provides a principled means of deciding when higher scales are more informative (emergence) or when higher scales are extraneous, epiphenomenal, or lossy (reduction).

Bringing these issues to network science, we can now ask: what representation will minimize the uncertainty present in a network? We do this by examining *causal emergence*, which is when a dimensionally-reduced network contains more informative dependencies, in the form of a higher EI than the original network. This phenomenon can be measured by recasting networks at higher scales and observing how the

EI changes, a process which identifies whether the network’s higher scales actually add information above and beyond lower scales.

Network macroscales

First we must introduce how to recast a network, G , at a higher scale. This is represented by a new network, G_M . Within G_M , a micro-node is a node that was present in the original G , whereas a macro-node is defined as a node, v_M , that represents a subgraph, S_i , from the original G (replacing the subgraph within the network). Since the original network has been dimensionally reduced by grouping nodes together, G_M will always have fewer nodes than G .

A macro-node μ is defined by some W_μ^{out} , derived from the edge weights of the various nodes within the subgraph it represents. One can think of a macro-node as being a summary statistic of the underlying subgraph’s behavior, a statistic that takes the form of a single node. Ultimately there are many ways of representing a subgraph, that is, building a macro-node, and some ways are more accurate than others in capturing the subgraph’s behavior, depending on the connectivity. To decide whether or not a macro-node is an accurate summary of its underlying subgraph, we check whether random walkers behave identically on G and G_M . We do this because many important analyses and algorithms—such as using PageRank for determining a node’s centrality [25] or InfoMap for community discovery [26]—are based on random walking.

Specifically, we define the *inaccuracy* of a macroscale as the Kullback-Leibler divergence [27] between the expected distribution of random walkers on G vs. G_M , given some identical initial distribution on each. The expected distribution over G at some future time t is $P_m(t)$, while the distribution over G_M at some future time t is $P_M(t)$. To compare the two, the distribution $P_m(t)$ is summed over the same nodes in the macroscale G_M , resulting in the distribution $P_{M|m}(t)$ (the microscale given the macroscale). We can then define the macroscale inaccuracy over some series of time steps T as:

$$\text{inaccuracy} = \sum_{t=0}^T D_{KL}[P_M(t)||P_{M|m}(t)] \quad (6)$$

This measure addresses the extent to which a random dynamical process on the microscale topology will be recapitulated on a dimensionally-reduced topology (for how this is applied in our analysis, see Materials & Methods).

What constitutes an accurate macroscale depends on the connectivity of the subgraph that gets grouped into a macro-node, as shown in Fig 4. The W_μ^{out} can be constructed based on the collective W^{out} of the subgraph (shown in Fig 4A). For instance, in some cases one could just coarse-grain a subgraph by using its average W^{out} as the W_μ^{out} of some new macro-node μ (as in Fig 4B). However, it may be that the subgraph has dependencies not captured by such a coarse-grain. Indeed, this is similar to the recent discovery that when constructing networks from data it is often necessary to explicitly model higher-order dependencies by using higher-order nodes so that the dynamics of random walks to stay true to the original data [28]. We therefore introduce *higher-order macro-nodes* (HOMs), which draw on similar techniques to accurately represent subgraphs as single nodes.

Different subgraph connectivities require different types of HOMs to accurately represent. For instance, HOMs can be based on the input weights to the macro-node, which take the form $\mu|j$. In these cases the $W_{\mu|j}^{out}$ is a weighted average of each node’s W^{out} in the subgraph, where the weight is based on the input weight to each node in the subgraph (as in Fig 4C). Another type of HOM that generally leads to accurate macro-nodes over time is when the W_μ^{out} is based on the stationary output from the subgraph to the rest of the network, which we represent as $\mu|\pi$ (Fig 4D). These types of HOMs may sometimes have minor inaccuracies given some initial state, but will almost always trend toward perfect accuracy as the network approaches its stationary dynamics (as outlined in the Materials & Methods section).

Subgraphs with complex internal dynamics can require a more complex type of HOM in order to preserve the network’s accuracy. For instance, in cases where subgraphs have a delay between their inputs and outputs, this can be represented by a combination of $\mu|j$ and $\mu|\pi$, which when combined captures that delay (Fig 4E). In these cases the macro-node μ has two components, one of which acts as a buffer over a timestep.

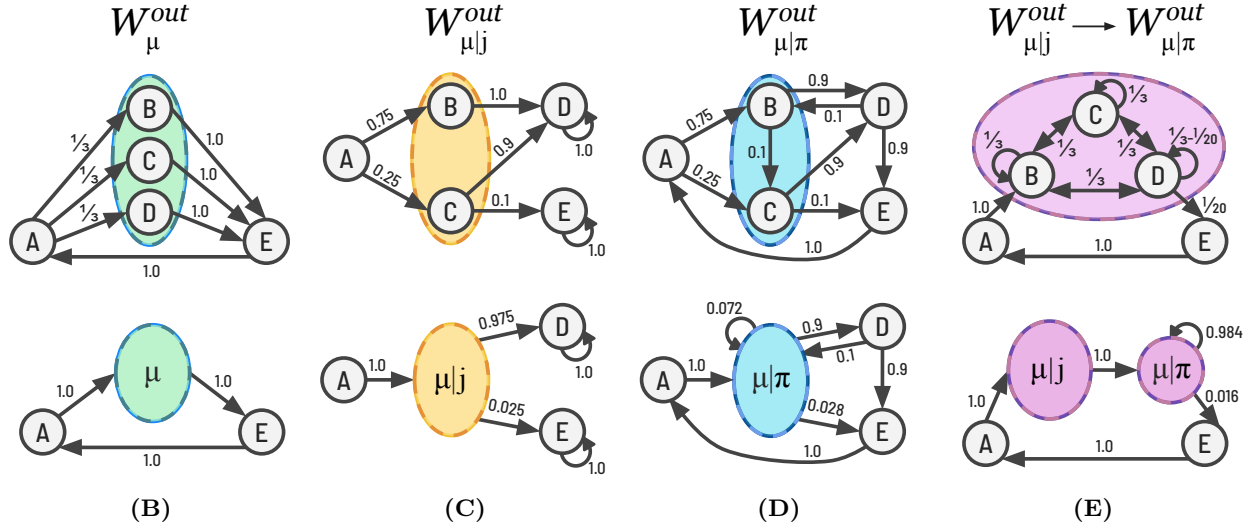
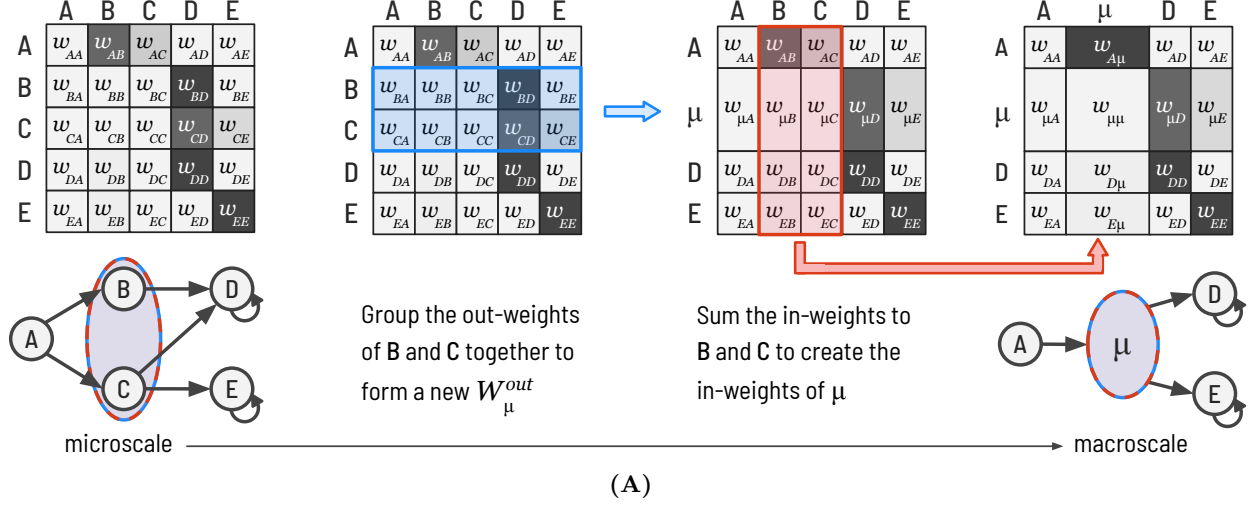


Figure 4: Macro-nodes. (A) The original network, G along with its adjacency matrix (left). The shaded oval indicates that subgraph S member nodes v_B and v_C will be grouped together, forming a macro-node, μ . All macro-nodes are some transformation of the original adjacency matrix via recasting it as a new adjacency matrix (right). The manner of this recasting depends on the type of macro-node. (B) The simplest form of a macro-node is when W_μ^{out} is an average of the W_i^{out} of each node in the subgraph. (C) A macro-node that represents some path-dependency, such as input from A . Here, in averaging to create the W_μ^{out} the out-weights of nodes v_B and v_C are weighted by their input from v_A . (D) A macro-node that represents the subgraph's output over the network's stationary dynamics. Each node has some associated π_i , which is the probability of v_i in the stationary distribution of the network. The W_μ^{out} of a $\mu|\pi$ macro-node is created by weighting each W_i^{out} of the micro-nodes in the subgraph S by $\frac{\pi_i}{\sum_{k \in S} \pi_k}$. (E) A macro-node with a single timestep delay between input $\mu|j$ and its output $\mu|\pi$, each constructed using the same techniques as its components. However, $\mu|j$ always deterministically outputs to $\mu|\pi$. See SM 1.1 for the full equations governing the creation of the W_μ^{out} of each of the different HOMs shown.

This means that macro-nodes can possess memory even when constructed from networks that are at the microscale memoryless, and in fact this type of HOM is sometimes necessary to accurately capture the microscale dynamics.

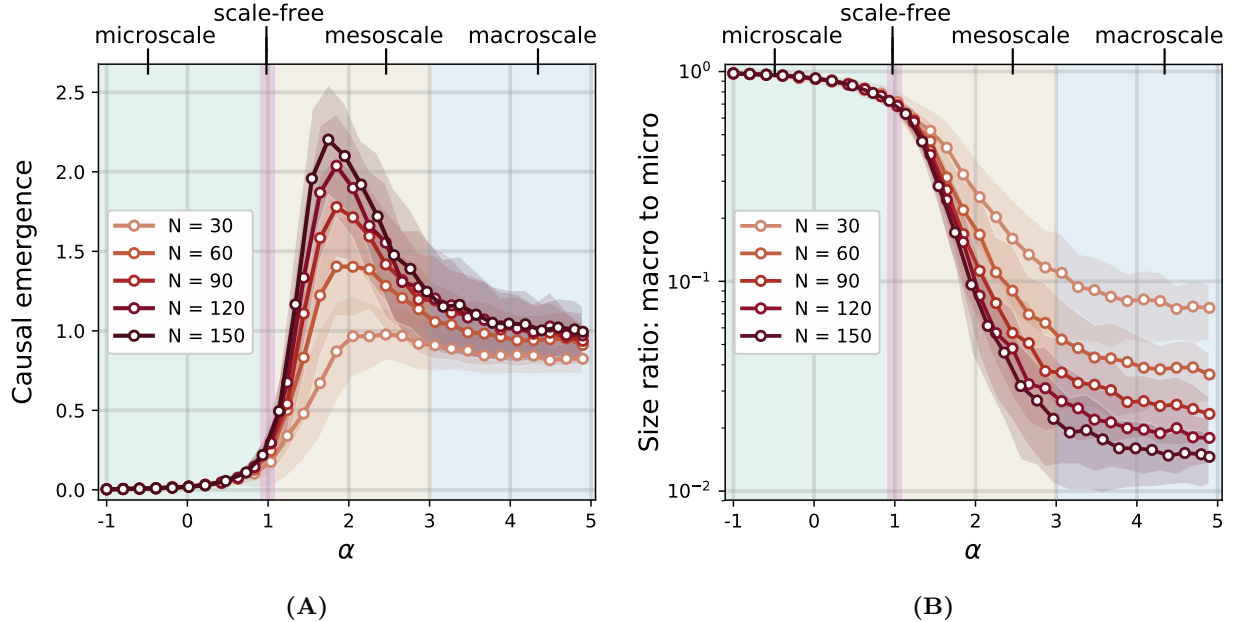


Figure 5: The emergence of scale in preferential attachment networks. (A) By repeatedly simulating networks with different degrees of preferential attachment (α values) with $m = 1$ new edge per each new node, and running them through a greedy algorithm (described in Materials & Methods), we observe a distinctive peak of causal emergence once the degree of preferential attachment is above $\alpha = 1$, yielding networks that are no longer “scale-free.” (B) The log of the ratio of original network size, N , to the size of the macroscale network, N_M . Networks with higher α values—more star-like networks—show drastic dimension reductions, and in fact all eventually reach the same N_M of 2. Comparatively, random trees ($\alpha = 0.0$) show essentially no informative dimension reductions.

We present these types of macro-nodes not as an exhaustive list of all possible HOMs, but rather as examples of how to construct higher scales in a network by representing subgraphs as nodes, and also sometimes using higher-order dependencies to ensure those nodes are accurate. This approach offers a complete generalization of previous work on coarse-grains [12] and also black boxes [29, 24, 30], while simultaneously solving the previously unresolved issue of macroscale accuracy by using higher-order dependencies. The types of macro-nodes formed by subgraphs also provides substantive information about the network, such as whether the macroscale of a network possesses memory or path-dependency.

Causal emergence reveals the scale of networks

Causal emergence occurs when a recast network, G_M (a macroscale), has more EI than the original network, G (the microscale). In general, networks with lower effectiveness (low EI given their size) have a higher potential for causal emergence, since they can be recast to reduce their uncertainty. Searching across groupings allows the identification or approximation of a macroscale that maximizes the EI .

Checking all possible groupings is computationally intractable for all but the smallest networks. Therefore, in order to find macro-nodes which increase the EI , we use a greedy algorithm that groups nodes together and checks if the EI increases. By choosing a node and then pairing it iteratively with its surrounding nodes we can grow macro-nodes until pairings no longer increase the EI , and then move on to a new node (see the Materials & Methods section for details on this algorithm).

By generating undirected preferential attachment networks and varying the degree of preferential attachment, α , we observe a crucial relationship between preferential attachment and causal emergence. One of

the central results in network science has been the identification of “scale-free” networks [18]. Our results show that networks that are not “scale-free” can be further separated into micro-, meso-, and macroscales depending on their connectivity. This scale can be identified based on their degree of causal emergence (Fig 5A). In cases of sublinear preferential attachment ($\alpha < 1.0$) networks lack higher scales. Linear preferential attachment ($\alpha = 1.0$) produces networks that are scale-free, which is the zone of preferential attachment right before the network develops higher scales. Such higher scales only exist in cases of superlinear preferential attachment ($\alpha > 1.0$). And past $\alpha > 3.0$ the network begins to converge to a macroscale where almost all the nodes are grouped into a single macro-node. The greatest degree of causal emergence is found in mesoscale networks, which is when α is between 1.5 and 3.0, when networks possess a rich array of macro-nodes.

Correspondingly the size of G_M decreases as α increases and the network develops an informative higher scale, which can be seen in the ratio of macroscale network size, N_M , to the original network size, N (Fig 5B). As discussed in previous sections, on the upper end of the spectrum of α the resulting network will approximate a hub-and-spoke, star-like network. Star-like networks have higher degeneracy and thus less EI , and because of this, we expect that there are more opportunities to increase the network’s EI through grouping nodes into macro-nodes. Indeed, the ideal grouping of a star network is when $N_M = 2$ and EI is 1 bit. This result is similar to recent advances in spectral coarse-graining that also observe that the ideal coarse-graining of a star network is to collapse it into a two-node network, grouping all the spokes into a single macro-node [31], which is what happens to star networks that are recast as macroscales.

Our results offer a principled and general approach to such community detection by asking when there is an informational gain from replacing a subgraph with a single node. Therefore we can define *causal communities* as being when a cluster of nodes, or some subgraph, forms a viable macro-node. Fundamentally causal communities represent noise at the microscale. The closer a subgraph is to complete noise, the greater the gain in EI by replacing it with a macro-node (see SM 1.7). Minimizing the noise in a given network also identifies the optimal scale to represent that network. However, there must be some structure that can be revealed by noise minimization in the first place. In cases of random networks that form a single large component which lacks any such structure, causal emergence does not occur (as shown in SM 1.7).

Causal emergence in real networks

The presence and informativeness of macroscales should vary across real networks, dependent on connectivity. Here we investigate the disposition toward causal emergence of real networks across different domains. We draw from the same set of networks that are analyzed in Fig. 3, the selection process and details of which is outlined in the Materials & Methods section. The network sizes span up to 40,000 nodes, thus making it unfeasible to find the the best macroscales for each of them. Therefore, we focus specifically on the two categories that previously showed the greatest divergence in terms of the EI : biological and technological. Since we are interested in the general question of whether biological or technological networks show a greater disposition or propensity for causal emergence, we approximate causal emergence by calculating the causal emergence of sampled subgraphs of growing sizes. Each sample is found using a “snowball sampling” procedure, wherein a node is chosen randomly and then a weakly connected subgraph of a specified size is found around it [32]. This subgraph is then analyzed using the previously described greedy algorithmic approach to find macro-nodes that maximized the EI in each network. Each available network is sampled 20 times for each size taken from it. In Figure 6, we show how the causal emergence of these real networks differentiates as we increase the sampled subgraph size, in a sequence of 50, 100, 150, and finally 200 nodes per sample. Networks of these sizes previously provided ample evidence of causal emergence in simulated networks, as in Fig. 5A. Comparing the two categories of real networks, we observe a significantly greater propensity for causal emergence in biological networks, and that this is more articulated the larger the samples are. Note that constructing a random null model of these networks (e.g., a configuration model) would tend to create networks with minimal or negligible causal emergence, as is the case for ER networks (Fig. 13 in SM 1.7).

That subsets of biological systems show a high disposition toward causal emergence is consistent, and even explanatory, of many long-standing hypotheses surrounding the existence of noise and degeneracy in biological systems [33]. It also explains the difficulty of understanding how the causal structure of biological systems function, since they are cryptic by containing certainty at one level and uncertainty at another.

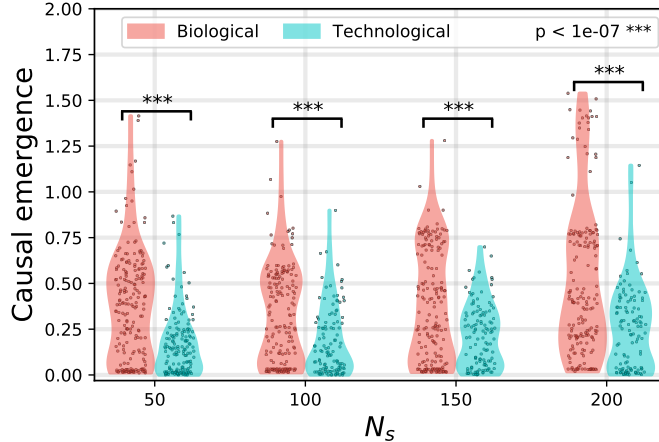


Figure 6: Propensity for causal emergence in real networks. Growing snowball samples of the two network domains that previously showed the greatest divergence in *effectiveness*: technological and biological networks. At each snowball size, N_s , each network is sampled 20 times. Across these samples the total amount of causal emergence for a given sample size is significantly different between the two domains (t-test, comparison of means).

Discussion

We have shown that the information in the dependencies between nodes in a network is a function of the uncertainty intrinsic to their connectivity, as well as how that uncertainty is distributed. To capture this information we adapted a measure, effective information (EI), for use in networks, and analyzed what it reveals about common network structures that have been studied by network scientists for decades. For example, the EI of an ER random network tends to $-\log_2(p)$, and whether the EI of a preferential attachment network grows or shrinks as new nodes are added is a function of whether its degree of preferential attachment, α , is greater or less than 1.0. In real networks, we showed that the EI of biological networks tends to be much lower than technological networks. Note that while EI can be used to analyze any network, in order to give its interpretation validity one should know whether the nodes and edges of a network represent actual dependencies such as causal relationships.

We also illustrated that causal emergence can occur in networks. Causal emergence is the gain in EI that occurs when a network, G , is recast as a new network, G_M . Finding an informative higher scale means balancing the minimization of uncertainty while simultaneously maximizing the number of nodes in the network. These methods may be useful in improving scientific experimental design, the compression and search of big data, model choice, and even machine learning. Importantly, not every recast network, G_M , will have a higher EI than the G that it represents, that is, these same techniques can identify cases of causal reduction. Ultimately, this is because comparing the EI of different network representations provides a ground for comparing the effectiveness of any two network representations of the same complex system. These techniques allow for the formal identification of the scale of a network. Scale-free networks can be thought of as possessing a fractal pattern of connectivity [34], and our results show that the scale of a network is the breaking of that fractal in one direction or the other.

The study of higher-order structures in networks is an increasingly rich area of research [26, 35, 36, 37, 38], often focusing on constructing networks that better capture the data they represent. Here we introduce a formal and generalized way to recast networks at a higher scales while preserving random walk dynamics. In many cases, a macroscale of a network can be just as accurate in terms of random walk dynamics and also possess greater EI . Some macro-nodes in a macroscale may be of different types with different higher-order properties. In other words, we show how to turn a lower-order network into a higher-order network.

One noteworthy and related aspect of our work is demonstrating how a system that is memoryless at the microscale can actually possess memory at the macroscale, indicating that whether a system has memory is a function of scale.

While some [39] have previously recast subgraphs as individual nodes as we do here, they have not done so in ways that are based on noise minimization and accuracy preservation, focusing instead on gains to algorithmic speed via compression. Explicitly creating macro-nodes to minimize noise brings the dependencies of the network into focus. This means that causal emergence in networks has a direct relationship to community detection, a vast sub-discipline that treats dense subgraphs within a network as representing shared properties, membership, or functions [40, 41]. Macro-nodes offer a *causal* community detection where the micro-nodes that make up a macro-node are a community, and ultimately can be replaced by a macro-node that summarizes their behavior while reducing the subgraph’s noise. Under this interpretation, community structure is characterized by noise rather than shared memberships. Since many networks possess hierarchies across scales [42], in the future these methods can be used to unravel the hierarchical multi-scale nature of networks in a principled manner based on noise reduction.

Materials & Methods

Selection of real networks

Networks were chosen to represent the four categories of interest: social, informational, biological, and technological (see SM Figure 10, where we detail the same information as in Figure 3, but also include the source of the network data in addition to the effectiveness value of each network). We used all the available networks under 40,000 nodes (due to computational constraints) within all the domains in the Konect database that reflected our categories of interest. For our social category we used the domains *Human Contact*, *Human Social*, *Social*, and *Communication*. For our information category we used the domains *Citations*, *Co-authorship*, *Hyperlinks*, *Lexical*, and *Software*. For our biological category we used the domains *Trophic* and *Metabolic*. Due to overlaps between the Konect database and the Network Repository [21] in these domains, and the paucity of other biological data in the Konect database, we also included the *Brains* domain and the *Ecology* domain from the Network Repository to increase our sample size (again, all networks within these domains under 40,000 nodes were included). For our technological category, we used the domains *Computer* and *Infrastructure* from the Konect database. Again due to overlap between the Konect database and the Network Repository, we also included the *Technological* and *Power Networks* domains from the Network Repository. For a full table of the networks used in this study, along with their source and categorization, see Table 2.

Creating accurate macro-nodes

Previously we outlined methods for creating accurate macro-nodes of different types. Here we explore their implementation, which requires deciding which macroscales are accurate. Accuracy is measured as the Kullback-Leibler divergence between the expected distribution of random walkers on both the microscale (G) and the macroscale (G_M), given an initial distribution, as in Eq. 6.

To measure the accuracy we use an initial maximum entropy distribution on the shared nodes between G and G_M . That is, only the set of nodes that are left ungrouped in G_M . Similarly, we only analyze the expected distribution over that same set of micro-nodes. Since such distributions are only over a portion of the network, to normalize each distribution to 1.0 we include a single probability that represents all the non-shared nodes between G and G_M (representing when a random walker is on a macro-node).

We focus on the shared nodes between G and G_M for the accuracy measure because: a) it is easy to calculate which is necessary during an algorithmic search, b) except for unusual circumstances the accuracy over the shared nodes still reflects the network as a whole, and c) even in cases of the most extreme macroscales (such as when $\alpha > 4$ in Fig 5), there are still nodes shared between G and G_M .

Here we examine our methods of using higher-order dependencies in order to demonstrate that this creates accurate macro-nodes. We use 1000 simulated preferential attachment networks, which were chosen as a uniform random sample between parameters $\alpha = 1.0$ and 2.0 , $n = 25$ to 35 , and with either $m = 1$ or 2 . These networks were then grouped via the algorithm described in the following section. All macro-nodes were of the $\mu|\pi$ type and their accuracy was checked over 1000 timesteps. These macro-nodes generally have accurate dynamics, either because they start that way or because they trend to that over time, and of the 1000 networks, only 4 had any divergence greater than 0 after 1000 timesteps. In Figure 11 in SM 1.6, we show 15 of these simulated networks, along with their parameters, number of macro-nodes, and inaccuracies. Note that even in the cases with early nonzero inaccuracy, this is always very low in absolute terms of bits, and of the randomly chosen 15 none do not trend toward accuracy over time. In our observations most macro-nodes converge before 500 timesteps, so therefore, in analyzing the real world networks using the $\mu|\pi$ macro-node we check all macro-nodes for accuracy and only reject those that are inaccurate at 500 timesteps. More details about the algorithmic approach to finding causal emergence is in the following section.

Greedy algorithm for causal emergence

The greedy algorithm used for finding causal emergence in networks is structured as follows: for each node, v_i , in the shuffled node list of the original network, collect a list of neighboring nodes, $\{v_j\} \in B_i$, where B_i is the *Markov blanket* of v_i (in graphical models, the Markov blanket, B_i , of a node, v_i , corresponds to the “parents”, the “children”, and the “parents of the children” of v_i [43]). This means that $\{v_j\} \in B_i$ consists of nodes with outgoing edges leading into v_i , nodes that the outgoing edges from v_i lead into, and nodes that have outgoing edges leading into the out-neighbors of v_i . For each node in $\{v_j\}$, the algorithm calculates the *EI* of a macroscale network after v_i and v_j are combined into a macro-node, v_M , according to one of the macro-node types in Figure 4. If the resulting network has a higher *EI* value, the algorithm stores this structural change and, if necessary, supplements the queue of nodes, $\{v_j\}$, with any new neighboring nodes from v_j ’s Markov blanket that were not already in $\{v_j\}$. If a node, v_j , has already been combined into a macro-node via a grouping with a previous node, v_i , then it will not be included in new queues, $\{v_j\}$, of later nodes to check. The algorithm iteratively combines such pairs of nodes until every node, v_j , in every node, v_i ’s Markov blanket is tested.

When examining an individual macro-node for whether it improves the *EI*, we default to the macro-type $\mu|\pi$ to save computational time, and check if there are any inaccuracies at 500 timesteps (if a macro-node generates inaccuracies, it is rejected). The accuracy measure is described in the Network Macroscales section.

Additional Information

Acknowledgements

Funding: This research was supported by the Allen Discovery Center program through The Paul G. Allen Frontiers Group (12171). This publication was made possible through the support of a grant from Templeton World Charity Foundation, Inc. (TWCFG0273). The opinions expressed in this publication are those of the author(s) and do not necessarily reflect the views of Templeton World Charity Foundation, Inc. This work was also supported in part by the National Defense Science & Engineering Graduate Fellowship (NDSEG) Program. **Author contributions:** B.K. and E.H. conceived the project. B.K. and E.H. wrote the article. B.K. performed the analyses. **Competing interests:** The authors declare no competing interests. The authors thank Conor Heins, Harrison Hartle, and Alessandro Vespignani for their insights about notation and formalism of effective information.

Data availability

All data used in this work was retrieved from the Konect Database [20] and also the Network Repository [21], which are publicly available. Software for calculating *EI* in networks and for finding causal emergence in networks is available by request (or upon publication at <https://github.com/jkbren/ei-net>).

References

- [1] Albert-László Barabási. *Network Science*. Cambridge University Press, 2016. ISBN: 1107076269.
- [2] Mark E. J. Newman. *Networks: An Introduction*. Oxford University Press, 2010, pp. 1–784. ISBN: 9780191594175. DOI: [10.1093/acprof:oso/9780199206650.001.0001](https://doi.org/10.1093/acprof:oso/9780199206650.001.0001).
- [3] Luís A. Nunes Amaral and J. M. Ottino. “Complex networks”. In: *The European Physical Journal B - Condensed Matter* 38.2 (2004), pp. 147–162. ISSN: 1434-6028. DOI: [10.1140/epjb/e2004-00110-5](https://doi.org/10.1140/epjb/e2004-00110-5).
- [4] Nicola Perra et al. “Activity driven modeling of time varying networks”. In: *Scientific Reports* 2 (2012), pp. 1–7. ISSN: 20452322. DOI: [10.1038/srep00469](https://doi.org/10.1038/srep00469).
- [5] Danielle S. Bassett and Olaf Sporns. “Network neuroscience”. In: *Nature Neuroscience* 20.3 (2017), pp. 353–364. ISSN: 15461726. DOI: [10.1038/nn.4502](https://doi.org/10.1038/nn.4502).
- [6] Albert-László Barabási, Natali Gulbahce, and Joseph Loscalzo. “Network medicine: A network-based approach to human disease”. In: *Nature Reviews Genetics* 12.1 (2011), pp. 56–68. ISSN: 14710056. DOI: [10.1038/nrg2918](https://doi.org/10.1038/nrg2918).
- [7] Judea Pearl. “Causality”. In: *New York: Cambridge* (2000). DOI: [10.1017/CB09780511803161](https://doi.org/10.1017/CB09780511803161).
- [8] Judea Pearl. “Causal diagrams for empirical research”. In: *Biometrika* 82.4 (1995), p. 669. DOI: [10.1093/biomet/82.4.669](https://doi.org/10.1093/biomet/82.4.669).
- [9] Aneta Koseska and Philippe I. H. Bastiaens. “Cell signaling as a cognitive process”. In: *The EMBO Journal* 36.5 (2017), pp. 568–582. ISSN: 0261-4189. DOI: [10.15252/embj.201695383](https://doi.org/10.15252/embj.201695383).
- [10] Francisco A. Rodrigues et al. “The Kuramoto model in complex networks”. In: *Physics Reports* 610 (2016), pp. 1–98. ISSN: 03701573. DOI: [10.1016/j.physrep.2015.10.008](https://doi.org/10.1016/j.physrep.2015.10.008).
- [11] Claude E. Shannon. “A mathematical theory of communication”. In: *The Bell System Technical Journal* 27.July 1928 (1948), pp. 379–423. ISSN: 07246811. DOI: [10.1145/584091.584093](https://doi.org/10.1145/584091.584093).
- [12] Erik P. Hoel, Larissa Albantakis, and Giulio Tononi. “Quantifying causal emergence shows that macro can beat micro”. In: *Proceedings of the National Academy of Sciences* 110.49 (2013), pp. 19790–5. ISSN: 1091-6490. DOI: [10.1073/pnas.1314922110](https://doi.org/10.1073/pnas.1314922110).
- [13] Erik P. Hoel. “Agent Above, Atom Below: How Agents Causally Emerge from Their Underlying Microphysics”. In: *Wandering Towards a Goal: How Can Mindless Mathematical Laws Give Rise to Aims and Intention?* Ed. by Anthony Aguirre, Brendan Foster, and Zeeya Merali. Cham: Springer International Publishing, 2018, pp. 63–76. ISBN: 978-3-319-75726-1. DOI: [10.1007/978-3-319-75726-1_6](https://doi.org/10.1007/978-3-319-75726-1_6).
- [14] Giulio Tononi and Olaf Sporns. “Measuring information integration”. In: *BMC Neuroscience* 4.1 (2003), p. 31. ISSN: 14712202. DOI: [10.1186/1471-2202-4-31](https://doi.org/10.1186/1471-2202-4-31).
- [15] Paul Erdős and Alfréd Rényi. “On random graphs”. In: *Publicationes Mathematicae* 6 (1959), pp. 290–297. ISSN: 00029947. DOI: [10.2307/1999405](https://doi.org/10.2307/1999405).
- [16] Béla Bollobás. “The Evolution of Random Graphs”. In: *Transactions of the American Mathematical Society* 286.1 (1984), p. 257. ISSN: 00029947. DOI: [10.2307/1999405](https://doi.org/10.2307/1999405).
- [17] Charo I. Del Genio, Thilo Gross, and Kevin E. Bassler. “All scale-free networks are sparse”. In: *Physical Review Letters* 107.17 (2011), pp. 1–4. ISSN: 00319007. DOI: [10.1103/PhysRevLett.107.178701](https://doi.org/10.1103/PhysRevLett.107.178701).
- [18] Albert-László Barabási, Réka Albert, and Hawoong Jeong. “Mean-field theory for scale-free random networks”. In: *Physica A* 272.1 (1999), pp. 173–187. ISSN: 03784371. DOI: [10.1016/S0378-4371\(99\)00291-5](https://doi.org/10.1016/S0378-4371(99)00291-5).
- [19] Duncan J. Watts and Steven H. Strogatz. “Collective dynamics of ‘small-world’ networks”. In: *Nature* 393.6684 (1998), pp. 440–442. ISSN: 0028-0836. DOI: [10.1038/30918](https://doi.org/10.1038/30918).
- [20] Jérôme Kunegis. “KONECT - the Koblenz network collection”. In: *Proceedings of the 22nd International Conference on World Wide Web Companion* (2013), pp. 1343–1350. DOI: [10.1145/2487788.2488173](https://doi.org/10.1145/2487788.2488173).

- [21] Ryan A. Rossi and Nesreen K. Ahmed. “NetworkRepository: An interactive data repository with multi-scale visual analytics”. In: *Twenty-Ninth AAAI Conference on Artificial Intelligence* (2015), pp. 4292–4293.
- [22] G. M. Edelman and J. A. Gally. “Degeneracy and complexity in biological systems”. In: *Proceedings of the National Academy of Sciences* 98.24 (2001), pp. 13763–13768. ISSN: 0027-8424. DOI: [10.1073/pnas.231499798](https://doi.org/10.1073/pnas.231499798).
- [23] G. Tononi, O. Sporns, and G. M. Edelman. “Measures of degeneracy and redundancy in biological networks”. In: *Proceedings of the National Academy of Sciences* 96.6 (1999), pp. 3257–3262. ISSN: 0027-8424. DOI: [10.1073/pnas.96.6.3257](https://doi.org/10.1073/pnas.96.6.3257).
- [24] Erik P. Hoel. “When the map is better than the territory”. In: *Entropy* 19.5 (2017), p. 188. ISSN: 1099-4300. DOI: [10.3390/e19050188](https://doi.org/10.3390/e19050188).
- [25] Lawrence Page et al. “The PageRank citation ranking: Bringing order to the web”. In: *World Wide Web Internet And Web Information Systems* (1998). ISSN: 1752-0509. DOI: [10.1.1.31.1768](https://doi.org/10.1.1.31.1768).
- [26] Martin Rosvall and C. T. Bergstrom. “Maps of random walks on complex networks reveal community structure”. In: *Proceedings of the National Academy of Sciences* 105.4 (2008), pp. 1118–23. ISSN: 1091-6490. DOI: [10.1073/pnas.0706851105](https://doi.org/10.1073/pnas.0706851105).
- [27] Thomas M. Cover and Joy A. Thomas. *Elements of Information Theory*. John Wiley & Sons, 2012, pp. 1–748. ISBN: 9780471241959. DOI: [10.1002/047174882X](https://doi.org/10.1002/047174882X).
- [28] Jian Xu, Thanuka L. Wickramaratne, and Nitesh V. Chawla. “Representing higher-order dependencies in networks”. In: *Science Advances* 2.5 (2016), e1600028. DOI: [10.1126/sciadv.1600028](https://doi.org/10.1126/sciadv.1600028).
- [29] W. Ross Ashby. *An Introduction to Cybernetics*. Chapman & Hall Ltd., 1957.
- [30] William Marshall, Larissa Albantakis, and Giulio Tononi. “Black-boxing and cause-effect power”. In: *PLoS Computational Biology* 14.4 (2018), pp. 1–21. ISSN: 1553-7358. DOI: [10.1371/journal.pcbi.1006114](https://doi.org/10.1371/journal.pcbi.1006114).
- [31] Edward Laurence et al. “Spectral dimension reduction of complex dynamical networks”. In: *Physical Review X* 9.1 (2019), p. 011042. ISSN: 2160-3308. DOI: [10.1103/PhysRevX.9.011042](https://doi.org/10.1103/PhysRevX.9.011042).
- [32] Douglas D. Heckathorn and Christopher Cameron. “Network sampling: From snowball and multiplicity to respondent-driven sampling”. In: *Annual Review of Sociology* (2017). DOI: [10.1146/annurev-soc-060116-053556](https://doi.org/10.1146/annurev-soc-060116-053556).
- [33] Giulio Tononi, Gerald M. Edelman, and Olaf Sporns. “Complexity and coherency: Integrating information in the brain”. In: *Trends in Cognitive Sciences* 2.12 (1998), pp. 474–484. ISSN: 13646613. DOI: [10.1016/S1364-6613\(98\)01259-5](https://doi.org/10.1016/S1364-6613(98)01259-5).
- [34] Albert-László Barabási, Erzsébet Ravasz, and Tamas Vicsek. “Deterministic scale-free networks”. In: *Physica A* 299 (2001), pp. 559–564. ISSN: 1889898X. DOI: [https://doi.org/10.1016/S0378-4371\(01\)00369-7](https://doi.org/10.1016/S0378-4371(01)00369-7).
- [35] Austin R. Benson, David F. Gleich, and Jure Leskovec. “Higher-order organization of complex networks”. In: *Science* 353.6295 (2016), pp. 163–166. DOI: [10.1126/science.aad9029](https://doi.org/10.1126/science.aad9029).
- [36] Ingo Scholtes. “When is a network a network? Multi-order graphical model selection in pathways and temporal networks”. In: *Proceedings of the 23rd ACM SIGKDD International Conference on Knowledge Discovery and Data Mining* (2017), pp. 1037–1046. DOI: [10.1145/3097983.3098145](https://doi.org/10.1145/3097983.3098145).
- [37] Hao Yin, Austin R. Benson, and Jure Leskovec. “Higher-order clustering in networks”. In: *Physical Review E* 97.5 (2018), pp. 1–11. ISSN: 24700053. DOI: [10.1103/PhysRevE.97.052306](https://doi.org/10.1103/PhysRevE.97.052306).
- [38] Renaud Lambiotte, Martin Rosvall, and Ingo Scholtes. “From networks to optimal higher-order models of complex systems”. In: *Nature Physics* (2019). ISSN: 1745-2473. DOI: [10.1038/s41567-019-0459-y](https://doi.org/10.1038/s41567-019-0459-y).
- [39] Natalie Stanley et al. “Compressing networks with super nodes”. In: *Scientific Reports* 8.10892 (2018), pp. 1–14. ISSN: 2045-2322. DOI: [10.1038/s41598-018-29174-3](https://doi.org/10.1038/s41598-018-29174-3).

- [40] Santo Fortunato and Darko Hric. “Community detection in networks: A user guide”. In: *Physics Reports* 659 (2016), pp. 1–44. ISSN: 03701573. DOI: [10.1016/j.physrep.2016.09.002](https://doi.org/10.1016/j.physrep.2016.09.002).
- [41] Filippo Radicchi et al. “Defining and identifying communities in networks”. In: *Proceedings of the National Academy of Sciences* 101.9 (2004), pp. 2658–2663. ISSN: 0027-8424. DOI: [10.1073/pnas.0400054101](https://doi.org/10.1073/pnas.0400054101).
- [42] Aaron Clauset, Christopher Moore, and M. E. J. Newman. “Structural inference of hierarchies in networks”. In: *Statistical Network Analysis: Models, Issues, and New Directions* (2006), pp. 1–13. DOI: [10.1007/978-3-540-73133-7_1](https://doi.org/10.1007/978-3-540-73133-7_1).
- [43] Karl J. Friston. “Life as we know it.” In: *Journal of the Royal Society Interface* 10.86 (2013), p. 20130475. ISSN: 1742-5662. DOI: [10.1098/rsif.2013.0475](https://doi.org/10.1098/rsif.2013.0475).
- [44] Giulio Tononi. “An information integration theory of consciousness”. In: *BMC Neuroscience* 5 (2004), pp. 1–22. ISSN: 14712202. DOI: [10.1186/1471-2202-5-42](https://doi.org/10.1186/1471-2202-5-42).
- [45] David Balduzzi and Giulio Tononi. “Qualia: The geometry of integrated information”. In: *PLoS Computational Biology* 5.8 (2009). ISSN: 1553734X. DOI: [10.1371/journal.pcbi.1000462](https://doi.org/10.1371/journal.pcbi.1000462).
- [46] R. A. Fisher. “The Design of Experiments.” In: *The American Mathematical Monthly* 43.3 (1936), p. 180. ISSN: 00029890. DOI: [10.2307/2300364](https://doi.org/10.2307/2300364).

1 Supplementary Materials

1.1 Table of key terms

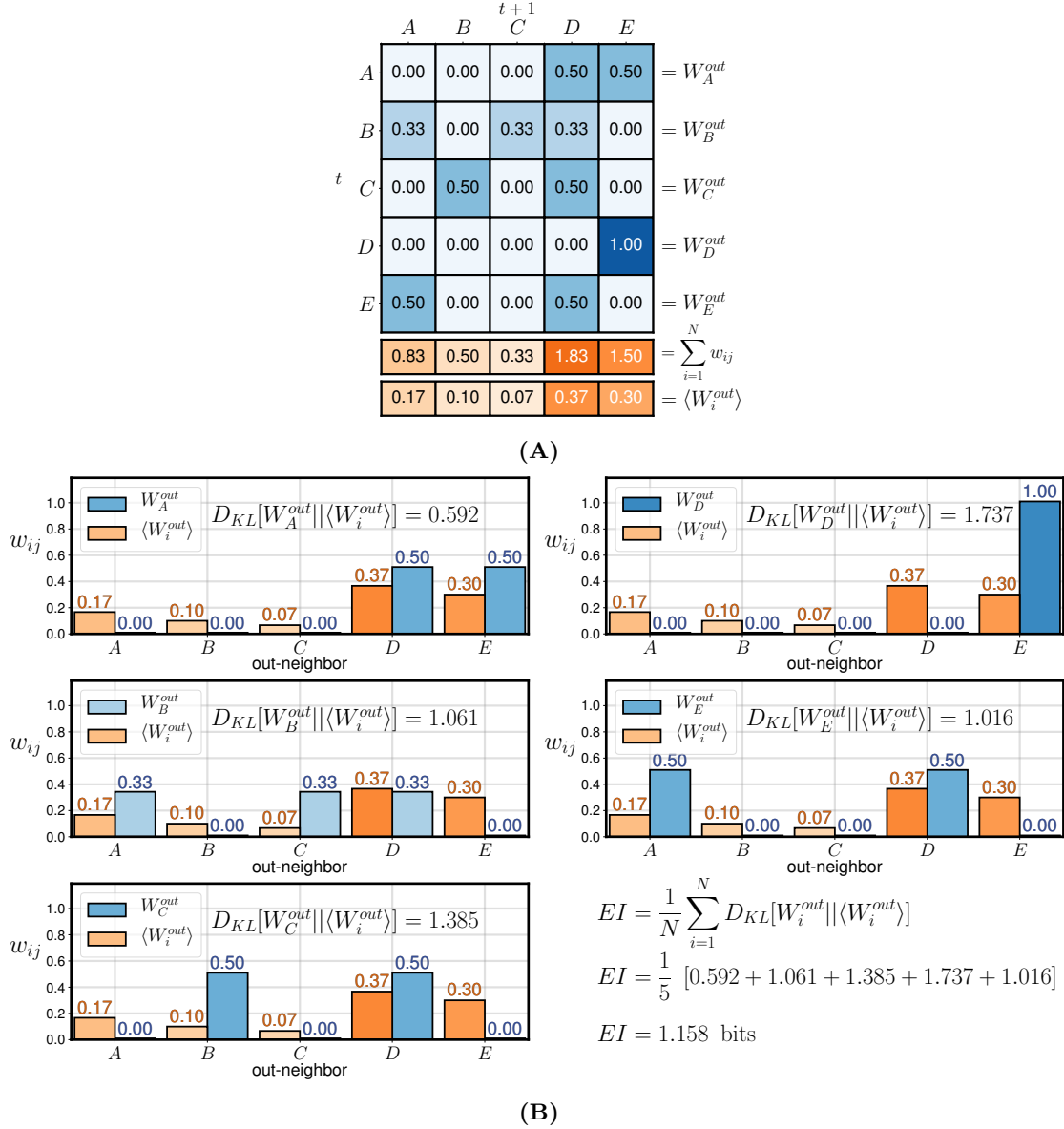
Term	Description	Notation
Network size	the number of nodes in the network	N
Out-weight vector (v_i)	a vector of probabilities w_{ij} that a random walker on node v_i will transition to v_j	$W_i^{out} = \{w_{i1}, w_{i2}, \dots, w_{ij}, \dots, w_{iN}\}$
Effective information (network)	the total information in a causal structure, in bits	$EI = H(\langle W_i^{out} \rangle) - \langle H(W_i^{out}) \rangle$
Determinism (v_i)	how certain about next steps is a random walker on v_i	$\det_i = \log_2(N) - H(W_i^{out})$
Degeneracy (network)	how distributed the certainty is over the nodes of the network	$\text{degeneracy} = \log_2(N) - H(\langle W_i^{out} \rangle)$
Effect information (v_i)	the contribution of each node v_i to the network's EI	$EI_i = D_{KL}[W_i^{out} \langle W_i^{out} \rangle]$
Micro-nodes in a macro-node	the set of micro-nodes grouped into a macro-node in the new network, G_M	$S = \{v_i, v_j, \dots\}$, of length N_S
Macro-node out-weights	the out-weights from macro-node, μ , to its neighbors	$W_\mu^{out} = \sum_{i \in S} W_i^{out} \cdot \left(\frac{1}{N_S}\right)$
Macro-node out-weights given input weights	the out-weights from macro-node, μ , to its neighbors, <i>conditioned</i> on in-weights to the micro-nodes, $v_i \in S$	$W_{\mu j}^{out} = \sum_{i \in S} W_i^{out} \cdot \left(\frac{\sum_{j \rightarrow i} w_{ji}}{\sum_{j \rightarrow k \in S} w_{jk}}\right)$
Macro-node out-weights given the stationary distribution	the out-weights from macro-node, μ , to its neighbors, <i>conditioned</i> on the stationary probabilities, π_i , of micro-nodes, $v_i \in S$	$W_{\mu \pi}^{out} = \sum_{i \in S} W_i^{out} \cdot \left(\frac{\pi_i}{\sum_{k \in S} \pi_k}\right)$

Table 1: Table of key terms. Listed above are the terms and quantities needed in order to calculate EI and create accurate macro-nodes.

1.2 Effective information calculation

Mathematically, EI has been expressed in a number of previous ways. The first was as the mutual information between two subsets of a system (while injecting noise into one), originally proposed as a step in the calculation of integrated information between neuron-like elements [44, 45]. More recently, it was pointed out that in general an intervention distribution, I_D , defined as a probability distribution over the $do(x)$ operator (as in [7]), creates some resultant effect distribution, E_D . Then the EI is the mutual information, $I(I_D; E_D)$, between the two, when the interventions are done like a randomized trial to reveal the dependencies (i.e., at maximum entropy [46, 24]).

In order to calculate the total information contained in the causal relationships of a system, EI is applied to the system as a whole [12]. There, EI was defined over the set of all states of a system and its state transitions. Because the adjacency matrix of a network can be cast as a transition matrix (as in Figure 7A),



$$EI = \frac{1}{N} \sum_{i=1}^N D_{KL}[W_i^{out} || \langle W_i^{out} \rangle]$$

$$EI = \frac{1}{5} [0.592 + 1.061 + 1.385 + 1.737 + 1.016]$$

$$EI = 1.158 \text{ bits}$$

Figure 7: Illustration of the calculation of effective information. (A) The adjacency matrix of a network with 1.158 bits of effective information (calculation shown in (B)). The rows correspond to W_i^{out} , a vector of probabilities that a random walker on node v_i at time t transitions to v_j in the following time step, $t + 1$. $\langle W_i^{out} \rangle$ represents the (normalized) input weight distribution of the network, that is, the probabilities that a random walker will arrive at a given node v_j at $t + 1$, after a uniform introduction of random walkers into the network at t . (B) Each node's contribution to the EI (EI_i) is the KL divergence of its W_i^{out} vector from the network's $\langle W_i^{out} \rangle$, known as the *effect information*.

the EI of a network can be expressed as:

$$EI = \frac{1}{N} \sum_{i=1}^N D_{KL}[W_i^{out} || \langle W_i^{out} \rangle] \quad (7)$$

where EI is the average of the *effect information*, EI_i , of each node (see Table 1 and Figure 7B). This is equivalent to our derivation of EI from first principles in Equation 1, since:

$$\begin{aligned}
EI &= \frac{1}{N} \sum_{i=1}^N D_{KL}[W_i^{out} || \langle W_i^{out} \rangle] = \frac{1}{N} \sum_{i=1}^N \sum_{j=1}^N w_{ij} \log_2 \left(\frac{w_{ij}}{W_j} \right) \\
&= \frac{1}{N} \sum_{i=1}^N \left(\sum_{j=1}^N w_{ij} \log_2(w_{ij}) - \sum_{j=1}^N w_{ij} \log_2(W_j) \right) \\
&= \frac{1}{N} \sum_{i=1}^N \sum_{j=1}^N w_{ij} \log_2(w_{ij}) - \frac{1}{N} \sum_{i=1}^N \sum_{j=1}^N w_{ij} \log_2(W_j) \quad (8)
\end{aligned}$$

Note that for a given node, v_i , the term in the first summation in Equation 8 above, $\sum_{j=1}^N w_{ij} \log_2(w_{ij})$, is equivalent to the negative entropy of the out-weights from v_i , $-H(W_i^{out})$. Also note that W_j , the j th element in the $\langle W_i^{out} \rangle$ vector, is the normalized sum of the incoming weights to v_j from its neighbors, v_i , such that $W_j = \frac{1}{N} \sum_{i=1}^N w_{ij}$. We substitute these two terms into Equation 8 above such that:

$$EI = \frac{1}{N} \sum_{i=1}^N -H(W_i^{out}) - \sum_{j=1}^N W_j \log_2(W_j)$$

This is equivalent to the formulation of EI from Equation 1, since $H(\langle W_i^{out} \rangle) = -\sum_{j=1}^N W_j \log_2(W_j)$:

$$EI = H(\langle W_i^{out} \rangle) - \langle H(W_i^{out}) \rangle \quad \square$$

In the derivations of SM 1.3 we adopt the relative entropy formulation of EI from Equation 7 for ease of derivation. For a visual intuition behind the calculations involved in this formulation of EI , see how the network in Figure 7A is used to calculate its EI (Figure 7B), by calculating the mean effect information, EI_i , of nodes in the network.

1.3 Deriving the effective information of common network structures

Here we inspect the EI for iconic graphical structures, and in doing so, we see several interesting relationships between a network structure and its EI . First, however, we will introduce key terminology and assumptions.

Let $\langle k \rangle$ be the average degree of a network, G , and each node, v_i , has degree, k_i . In directed graphs each v_i has an in-degree, k_i^{in} , and an out-degree, k_i^{out} . These correspond to the number of edges leading in to v_i and edges going out from v_i . The total number of edges in G is represented by E . In undirected Erdős-Rényi (ER) networks, the total number of edges is given by $E = p \frac{N(N-1)}{2}$, where p represents the probability that any two nodes, v_i and v_j , will be connected. In the following subsections, we derive the EI of several prototypical network structures, from random graphs to ring lattices to star networks. Note that for the following derivations we proceed from the relative entropy formalism from SM 1.2, and note that therefore N is the number of nodes with the output, $N = N_{out}$.

1.3.1 Derivation: effective information of ER networks

In Erdős-Rényi networks, EI does not depend on the number of nodes in the network, N . Instead, the network's EI reaches its maximum at $-\log_2(p)$. This is because in Erdős-Rényi networks, each node is

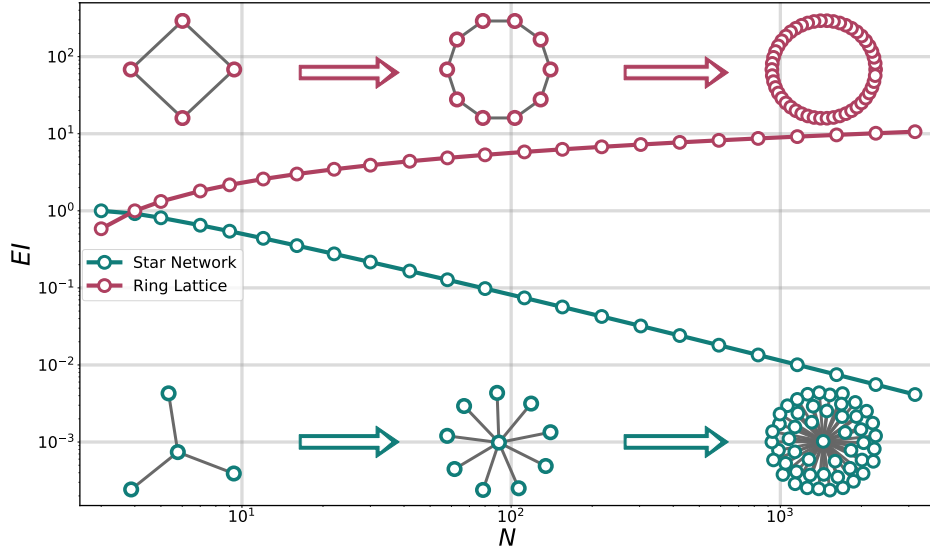


Figure 8: Effective information of stars and rings. As the number of nodes in star networks increases, we observe an EI that approaches zero, while the EI of ring lattice networks grows logarithmically as the number of nodes increases.

expected to connect to $\langle k \rangle = pN$ neighboring nodes, such that every value in $W_i^{out} = \frac{1}{\langle k \rangle}$ and every value in $\langle W_i^{out} \rangle = \frac{\langle k \rangle}{N \langle k \rangle} = \frac{1}{N}$, which can be represented as:

$$EI_{ER} = \frac{1}{N} \sum_i^N D_{KL} \left[\left(\frac{1}{\langle k \rangle}, \frac{1}{\langle k \rangle}, \dots \right) \parallel \left(\frac{1}{N}, \frac{1}{N}, \dots \right) \right] \quad (1)$$

Each node in an ER network is expected to be identical to all other nodes in the network, and calculating the expected *effect information*, EI_i , is equivalent to calculating the network's EI . As such, we observe:

$$EI_i = \sum_{j=1}^{k_i} \frac{1}{\langle k \rangle} \cdot \log_2 \left(\frac{\frac{1}{\langle k \rangle}}{\frac{1}{N}} \right) = \log_2 \left(\frac{N}{pN} \right) = EI_{ER} = \frac{1}{N} \cdot \sum_i^N -\log_2(p) = -\log_2(p)$$

1.3.2 Derivation: effective information of ring-lattice and star networks

Here, we compare two classes of networks with the same average degree—ring lattice networks and star, or hub-and-spoke, graphs. In each network, we assume an average degree $\langle k \rangle = 2d$, with d being the dimension. The EI of star network, EI_{star} , approaches 0.0 as N gets larger, while the EI of ring lattices approaches $\log_2(N) - \log_2(2d)$. These derivations are shown below, first for the d -dimensional ring lattice, EI_d .

As every node in a ring lattice is connected to its $2d$ neighbors, each element of $\langle W_i^{out} \rangle$ is $\frac{1}{2d}$ and each element of W^{in} is $\frac{2d}{2d \times N} = \frac{1}{N}$.

$$EI_d = \frac{1}{N} \cdot \sum_i D_{KL} \left[\left(\frac{1}{2d}, \frac{1}{2d}, \dots \right) \parallel \left(\frac{1}{N}, \frac{1}{N}, \dots \right) \right] \quad (11)$$

Each node in a d -dimensional ring lattice is expected to be identical, so calculating the expected *effect information*, EI_i , is equivalent to calculating the network's EI . As such, we observe:

$$EI_i = \sum_{j=1}^{2d} \frac{1}{2d} \cdot \log_2 \left(\frac{\frac{1}{2d}}{\frac{1}{N}} \right) = \log_2 \left(\frac{N}{2d} \right) = EI_d = \log_2(N) - \log_2(2d) \quad (12)$$

Note: the EI of ring lattice networks reduces to simply the *determinism* of the network. The EI of ring lattice networks scale logarithmically with the size of the network, which is contrasted by the behavior of EI in star networks. Star networks have a hub-and-spoke structure, where $N - 1$ nodes of degree $k_{spoke} = 1$ are connected a hub node, which itself has degree $k_{hub} = N - 1$. For star networks, EI approaches 0.0 as the number of nodes increases. This derivation is shown below.

$$EI_{star} = \frac{1}{N} \cdot \left[\sum_{i=1}^{N-1} D_{KL} [W_{spoke}^{out} || \langle W_i^{out} \rangle] + D_{KL} [W_{hub}^{out} || \langle W_i^{out} \rangle] \right]$$

Every spoke has an out-weight vector W_i^{out} with $N - 1$ elements of $w_{ij} = 0.0$ and one with $w_{ij} = 1.0$. The single hub, however, has $N - 1$ elements of $w_{ij} = \frac{1}{N-1}$ with a single $w_{ij} = 0.0$. Similarly, $\langle W_i^{out} \rangle$ consists of $N - 1$ elements with values $\frac{1}{N(N-1)}$.

$$EI_{star} = \frac{1}{N} \cdot \left[\sum_{i=1}^{N-1} D_{KL} \left[\frac{1}{1} || \frac{N-1}{N} \right] + D_{KL} \left[\frac{1}{N-1} || \frac{1}{N(N-1)} \right] \right] \quad (13)$$

Using the same techniques as above, this equation reduces to:

$$\begin{aligned} EI_{star} &= \frac{1}{N} \cdot \left[(N-1) \cdot \log_2 \left(\frac{\frac{1}{1}}{\frac{N-1}{N}} \right) + \log_2 \left(\frac{\frac{1}{N-1}}{\frac{1}{N(N-1)}} \right) \right] \\ EI_{star} &= \frac{N-1}{N} \cdot \log_2 \left(\frac{N}{N-1} \right) + \frac{1}{N} \cdot \log_2(N) \\ EI_{star} &= 0.0 \text{ as } \lim_{N \rightarrow \infty} \end{aligned} \quad (14)$$

1.4 Network motifs as causal relationships

It is important to understand why certain motifs have more EI while others have less. In Figure 9, we show the EI in 13 directed three-node network motifs. The connectivity of each motif drastically influences the EI . Motif 09—the directed cycle—is the motif with the highest EI . Intuitively, this fits with our definition of EI : the amount of certainty in the network (notably, each link in Motif 09, if taken to represent a causal relationship, is both necessary and sufficient). A random walker in this system has zero entropy (even if the direction of its path were reversed), whereas every other three-node motif does not contain that degree of certainty. Second, we see that Motif 04—a system with a “sink” node—has no EI , suggesting that a causal structure with that architecture is not informative, since all causes lead to the same effect. Similarly, because there are no outputs from two nodes in Motif 01, we see an EI value of zero.

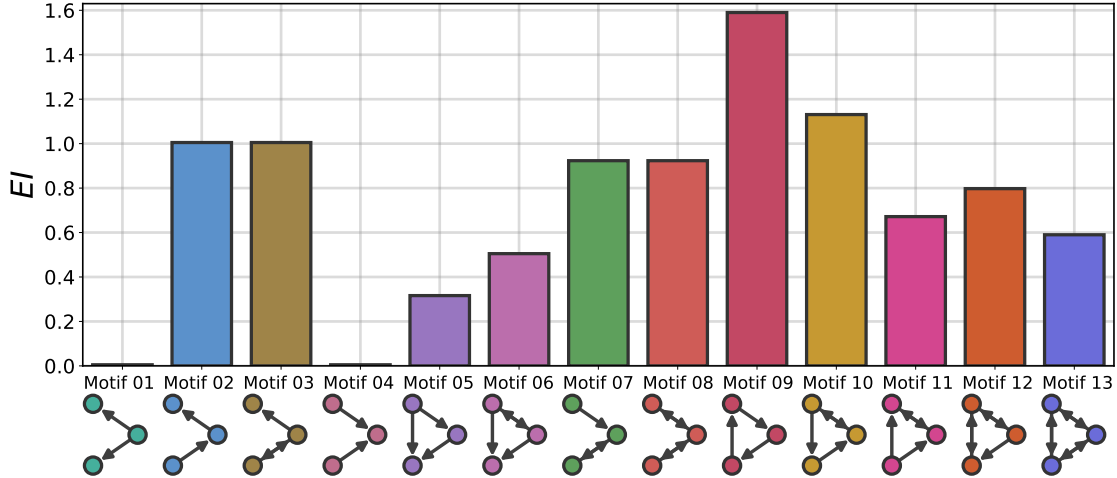


Figure 9: **Effective Information of network motifs.** All directed 3-node subgraphs and their EI .

1.5 Table of network data

In Table 2, we report the name, domain, source, category, and description of each of the 84 networks used in our comparison of EI in real networks. These networks were selected primarily from the Konect database [20], with supplemental datasets added from NetworkRepository [21] when the Konect database lacked a sufficient number of datasets in a given category, since the two databases already significantly overlapped. In many cases, the interactions among nodes in these networks (i.e., their edges) can reasonably be interpreted as causal, directed influence, or dependencies such that the behavior of a node, v_i , at a given time can be thought to impact the behavior of its neighbors, v_j . By instituting relatively minimal requirements for selecting the above networks, we are able to assess the EI in a variety of complex systems across different domains. However, while we can measure the EI of any given network, the further interpretation of this EI depends also on what the nodes and edges of a network represent. In a case where the nodes represent states of a system, such as a Markov process, then the EI directly captures the information in the causal structure. In the case where the nodes represent merely dependencies or influence, EI can still be informative as a metric to compare different networks. In a network specifically composed of non-causal correlations, then EI is merely a structural property of the network’s connectivity.

1.6 Examples of accurate macro-nodes

In Figure 11 we display 15 different parameterizations of small networks grown under degree-based preferential attachment. Each plot shows to the inaccuracy of the mapping from the microscale to the macroscale, in bits, which corresponds to the KL divergence of the distribution of random walkers on microscale nodes and the same distribution at the macroscale. Each of these networks are accurate after 1000 timesteps, with eight showing full accuracy from the start. These 15 example networks also show the range of causal emergence values that is found in networks.

1.7 Emergent subgraphs

What sort of subgraph connectivity leads to causal emergence? To explore this we take two independent subgraphs, and couple them together while varying their size, moving from clique-like to bipartite connectivity. We then check to see if grouping those clusters into macro-nodes leads to causal emergence (Figure 12). Specifically, we simulate many small unweighted, undirected networks ($N = 100$) from a stochastic block model with two clusters, and we vary the probability of within-cluster edges (from 0.0 to 1.0) as well

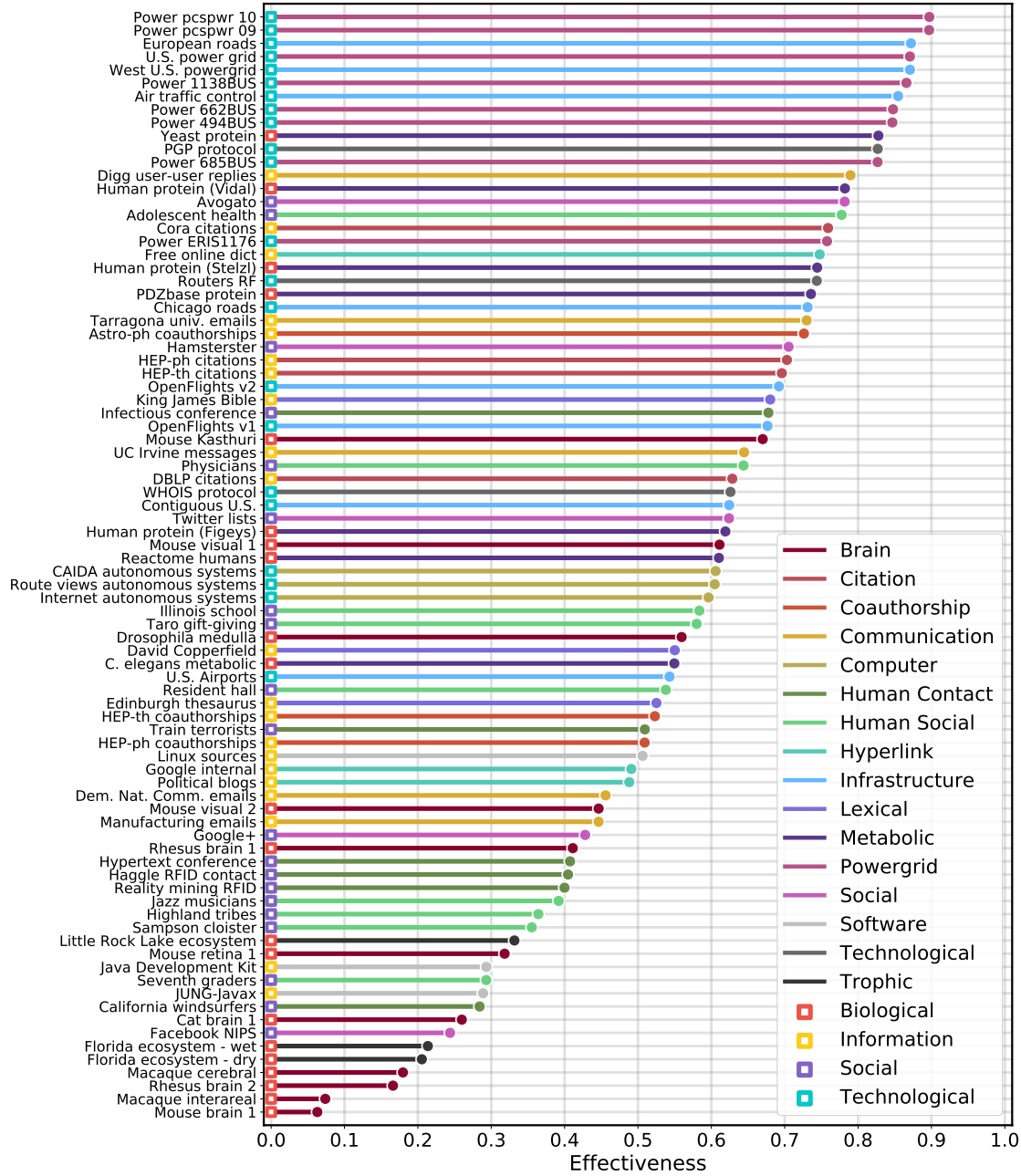


Figure 10: Effectiveness of real networks. Here, we report the full data behind the results summarized in Figure 3, color-coded in two ways. The first is by 16 “Domains” (as in Table 2), which corresponds to the classification of each network from its source repository (in this case, the Konect database [20] or the Network Repository [21]). The second categorization we report—those used in Figure 3—involves grouping the Domains into four “Categories” (“Cat.” in Table 2): Biological, Information, Social, and Technological. These correspond to the colored squares to the right of each network’s name.

as the size-asymmetry of the two clusters (illustrated around the border of Figure 12). In each simulation, we group the microscale network into two macro-nodes, each corresponding to one cluster. What we observe

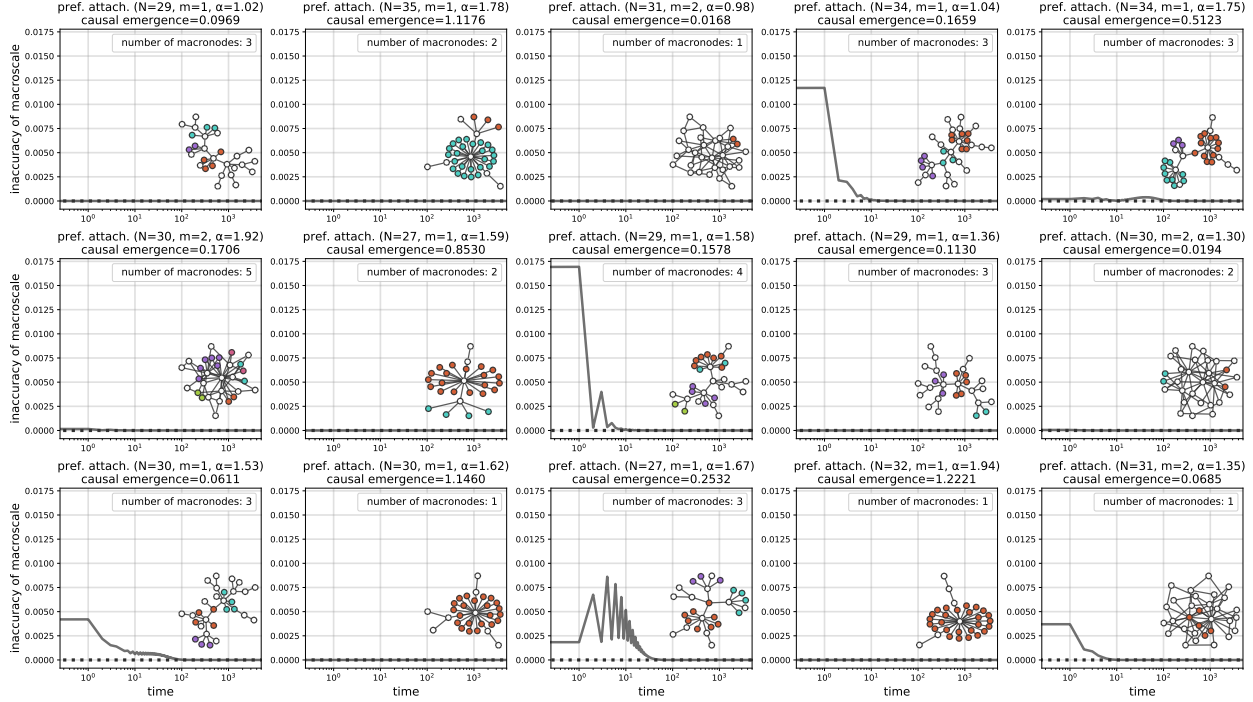


Figure 11: Typically minimal inaccuracies of higher-order macro-nodes. Each inset is of the microscale network, where each node’s color corresponds to the $\mu|\pi$ macro-node it has been mapped to following one instance of the greedy algorithm detailed in the Materials & Methods section. White nodes indicate a micro-node that was not grouped into a new macro-node. Inaccuracy is plotted over time.

is a causal emergence landscape with several important characteristics (Figure 12). First, in these networks we observe causal emergence when the fraction of within-cluster connections is either very high or very low (right and left sides of the heatmap in Figure 12). These are the conditions in which there is a large amount of uncertainty, or noise, in that subgraph. Not only that, however, causal emergence is most likely when there is a size asymmetry between the two clusters, suggesting that macroscales that maximize a network’s EI often do so by creating a more evenly distributed $\langle W_i^{out} \rangle$. In general, however, the space of subgraphs leans toward causal reduction (a loss of EI after grouping), which fits with the success of reduction historically and explains why researchers and modelers should generally be biased toward reduction.

In cases of complete noise, with no asymmetries or differences between intra- or inter-connectivity between subgraphs, we should expect causal emergence to be impossible. Indeed, this is what we see for many parameterizations of Erdős-Rényi networks of various sizes (Figure 13). This result follows from insights in Figure 1A, where the EI of ER networks converges to a fixed value of $-\log_2(p)$ as the size of the network increases. Here, we observe some causal emergence in ER networks but only when the networks are very small. Importantly, the amount of causal emergence is also very small, especially relative to the causal emergence in networks with preferential attachment. This further suggests that causal emergence moves the existent structure of the network into focus by examining the network at a certain scale, rather than creating that structure from nothing.

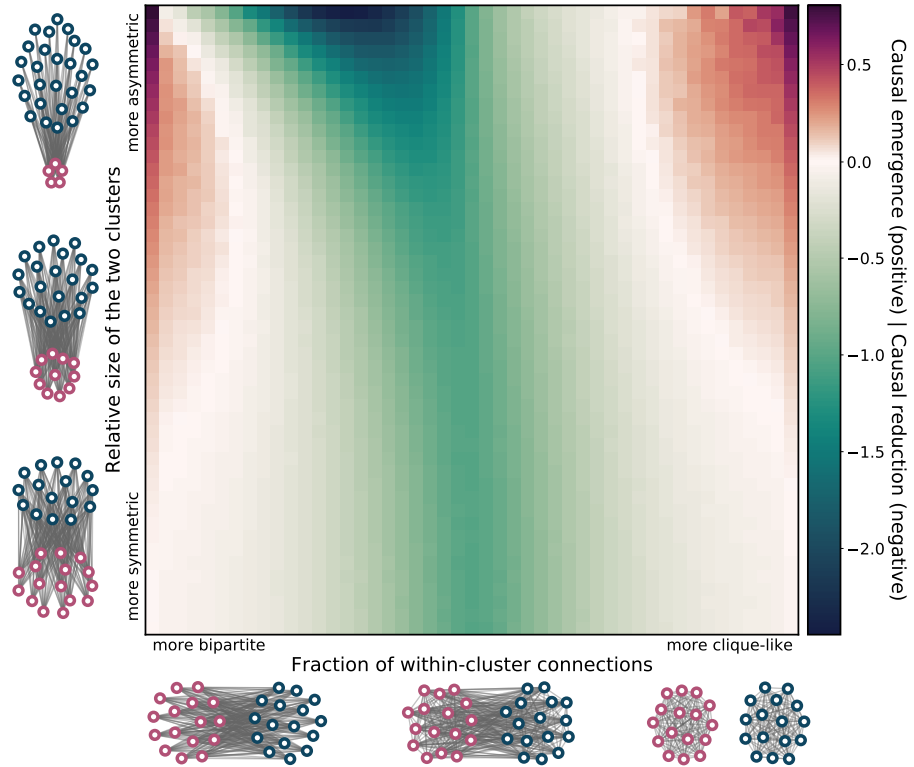


Figure 12: Causal emergence in a simplified stochastic block model. Schematic showing the role of the two relevant parameters—the fraction of nodes in each community (ranging from $r = 0.50$ to $r < 1.0$) and the fraction of within-cluster connections (ranging from $p = 0.0$, a fully bipartite network, to $p = 1.0$ —two disconnected cliques). By repeatedly simulating networks under various combinations of parameters ($N = 100$ with 100 simulations per combination of parameters), we see combinations that are more apt to produce networks that display causal emergence.

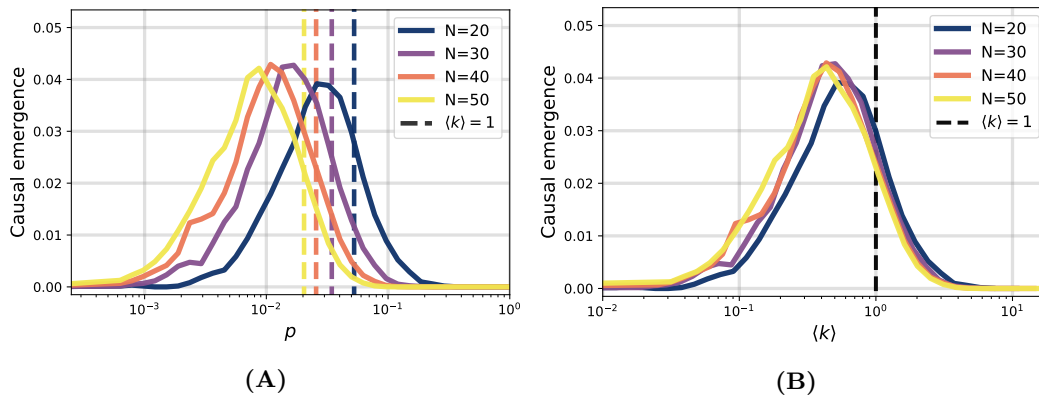


Figure 13: Causal emergence in Erdős-Rényi networks. (A) As the edge density, p , of ER networks increases and n is held constant, the amount of causal emergence quickly drops to zero. (B) This drop occurs well before $pN = \langle k \rangle = 1$, meaning the algorithm for uncovering causal emergence is only grouping small, disconnected, tree-like subgraphs that have yet to form into a giant randomly-connected component. Of note here is the low magnitude of causal emergence even in cases where the random network is not a single large component, and the vanishing of causal emergence after it is.

Network name	Domain	Source	Cat.	Description
HEP-th citations	Citation	Konect	Inf.	high-energy physics (HEP) citations - theory
HEP-ph citations	Citation	Konect	Inf.	HEP citations - phenomenology
Cora citations	Citation	Konect	Inf.	citations from the Cora database
DBLP citations	Citation	Konect	Inf.	database of scientific publications
Astro-ph coauthorships	Coauthorship	Konect	Inf.	coauthors on astronomy arXiv papers
HEP-th coauthorships	Coauthorship	Konect	Inf.	coauthors on HEP-theory arXiv papers
HEP-ph coauthorships	Coauthorship	Konect	Inf.	coauthors on HEP-phenomenology arXiv papers
Tarragona univ. emails	Communication	Konect	Soc.	emails from the University Rovira i Virgili
Dem. Nat. Comm. emails	Communication	Konect	Soc.	2016 Democratic National Committee email leak
Digg user-user replies	Communication	Konect	Soc.	reply network from the social news website Digg
UC Irvine messages	Communication	Konect	Soc.	messages between students at UC Irvine
Manufacturing emails	Communication	Konect	Soc.	internal emails between employees at a company
CAIDA autonomous systems	Computer	Konect	Tec.	autonomous systems network from CAIDA, 2007
Route views autonomous systems	Computer	Konect	Tec.	autonomous systems network
Internet autonomous systems	Computer	Konect	Tec.	connected IP routing
Haggle RFID contact	Human Contact	Konect	Soc.	human proximity, via carried wireless devices
Reality mining RFID	Human Contact	Konect	Soc.	RFID data from 100 MIT students' interactions
California windsurfers	Human Contact	Konect	Soc.	contacts between windsurfers California, 1986
Train terrorists	Human Contact	Konect	Soc.	contacts between Madrid train bombing suspects
Hypertext conference	Human Contact	Konect	Soc.	face-to-face contacts at the ACM Hypertext 2009
Infectious conference	Human Contact	Konect	Soc.	face-to-face contacts at INFECTIOUS, 2009
Jazz musicians	Human Social	Konect	Soc.	collaboration network between Jazz musicians
Adolescent health	Human Social	Konect	Soc.	surveyed students list their best friends
Physicians	Human Social	Konect	Soc.	innovation spread network among 246 physicians
Resident hall	Human Social	Konect	Soc.	friendship ratings between students in a dorm
Sampson cloister	Human Social	Konect	Soc.	relations between monks in a monastery
Seventh graders	Human Social	Konect	Soc.	proximity ratings between seventh grade students
Taro gift-giving	Human Social	Konect	Soc.	gift-givings (taro) between households
Dutch college	Human Social	Konect	Soc.	friendship ratings between university freshmen
Highland tribes	Human Social	Konect	Soc.	tribes in the Gahuku–Gama alliance structure
Illinois school	Human Social	Konect	Soc.	friendships between boys at an Illinois highschool
Free online dict.	Hyperlink	Konect	Inf.	cross references in Free Online Dict. of Computing
Political blogs	Hyperlink	Konect	Inf.	hyperlinks between blogs, 2004 US election
Google internal	Hyperlink	Konect	Inf.	hyperlink network from pages within Google.com
Air traffic control	Infrastructure	Konect	Tec.	USA's FAA, Preferred Routes Database
OpenFlights v1	Infrastructure	Konect	Tec.	flight network between airports, OpenFlights.org
OpenFlights v2	Infrastructure	Konect	Tec.	flight network between airports, OpenFlights.org
Contiguous U.S.	Infrastructure	Konect	Tec.	48 contiguous states and D.C. of the U.S.
European roads	Infrastructure	Konect	Tec.	international E-road network, mainly in Europe
Chicago roads	Infrastructure	Konect	Tec.	road transportation network of the Chicago region
West U.S. powergrid	Infrastructure	Konect	Tec.	power grid of the Western U.S.
U.S. Airports	Infrastructure	Konect	Tec.	flights between US airports in 2010
David Copperfield	Lexical	Konect	Inf.	network of common noun and adjective adjacencies
Edinburgh thesaurus	Lexical	Konect	Inf.	word association network, collected experimentally
King James Bible	Lexical	Konect	Inf.	co-occurrence between nouns in the Bible
C. elegans metabolic	Metabolic	Konect	Bio.	metabolic network of the <i>C. elegans</i> roundworm
Human protein (Figeys)	Metabolic	Konect	Bio.	interactions network of proteins in Humans
PDZbase protein	Metabolic	Konect	Bio.	protein–protein interactions from PDZBase
Human protein (Stelzl)	Metabolic	Konect	Bio.	interactions network of proteins in Humans
Human protein (Vidal)	Metabolic	Konect	Bio.	proteome-scale map of Human protein interactions
Yeast protein	Metabolic	Konect	Bio.	protein interactions contained in yeast
Reactome humans	Metabolic	Konect	Bio.	protein interactions, from the Reactome project

Table 2: Network datasets. Continued on the following page.

Network name	Domain	Source	Cat.	Description
Avogato	Social	Konect	Soc.	trust network for users of Advogato
Google+	Social	Konect	Soc.	Google+ user-user connections
Hamsterster	Social	Konect	Soc.	friendships between users of hamsterster.com
Twitter lists	Social	Konect	Soc.	Twitter user-user following network
Facebook NIPS	Social	Konect	Soc.	Facebook user-user friendship network
Linux dependency	Software	Konect	Inf.	Linux source code dependency network
J.D.K. dependency	Software	Konect	Inf.	software class dependencies, JDK 1.6.0.7
JUNG/javax dependency	Software	Konect	Inf.	software class dependencies, JUNG 2.0.1 & javax
Florida ecosystem - dry	Trophic	Konect	Bio.	food web in the Florida wetlands (dry season)
Florida ecosystem - wet	Trophic	Konect	Bio.	food web in the Florida wetlands (wet season)
Little Rock Lake ecosystem	Trophic	Konect	Bio.	food web of Little Rock Lake, Wisconsin
WHOIS protocol	Technological	NetworkRepository	Tec.	dataset of internet routing registries
PGP protocol	Technological	NetworkRepository	Tec.	trust protocol of private keys of internet users
Routers RF	Technological	NetworkRepository	Tec.	traceroute network between routers via Rocketfuel
Cat brain 1	Brain	NetworkRepository	Bio.	fiber tracts between brain regions of a cat
Drosophila medulla	Brain	NetworkRepository	Bio.	neuronal network from the medulla of a fly
Rhesus brain 1	Brain	NetworkRepository	Bio.	collation of tract tracing studies in primates
Rhesus brain 2	Brain	NetworkRepository	Bio.	inter-areal cortical networks from a primate
Macaque cerebral	Brain	NetworkRepository	Bio.	connections between cerebral cortex of a primate
Macaque interareal	Brain	NetworkRepository	Bio.	inter-areal cortical networks from a primate
Mouse Kasthuri	Brain	NetworkRepository	Bio.	neuronal network of a mouse
Mouse brain 1	Brain	NetworkRepository	Bio.	calcium imaging of neuronal networks in a mouse
Mouse retina 1	Brain	NetworkRepository	Bio.	electron microscopy of neurons in mouse retina
Mouse visual 1	Brain	NetworkRepository	Bio.	electron microscopy of visual cortex of a mouse
Mouse visual 2	Brain	NetworkRepository	Bio.	electron microscopy of visual cortex of a mouse
Power 1138BUS	Powergrid	NetworkRepository	Tec.	power system admittance, via Harwell-Boeing
Power 494BUS	Powergrid	NetworkRepository	Tec.	power system admittance, via Harwell-Boeing
Power 662BUS	Powergrid	NetworkRepository	Tec.	power system admittance, via Harwell-Boeing
Power 685BUS	Powergrid	NetworkRepository	Tec.	power system admittance, via Harwell-Boeing
U.S. power grid	Powergrid	NetworkRepository	Tec.	electricity / power transmission network in the U.S.
Power pcspwr 09	Powergrid	NetworkRepository	Tec.	BCSPWR09 powergrid data via Harwell-Boeing
Power pcspwr 10	Powergrid	NetworkRepository	Tec.	BCSPWR10 powergrid data via Harwell-Boeing
Power ERIS1176	Powergrid	NetworkRepository	Tec.	powergrid data via Erisman, 1973

Table 2: Network datasets (continued).